Università degli Studi di Firenze

Dipartimento di Matematica "Ulisse Dini"

Dottorato di Ricerca in Matematica

Hyperbolic 4-manifolds and the 24-cell

Leone Slavich

Tutor
Prof. Graziano Gentili

Coordinatore del Dottorato
Prof. Alberto Gandolfi

Relatore
Prof. Bruno Martelli

Ciclo XXVI, Settore Scientifico Disciplinare MAT/03

Contents

Chapter 1

Introduction

In the early 1980's, a major breakthrough in the field of low-dimensional topology was William P. Thurston's geometrization theorem for Haken manifolds [16] and the subsequent formulation of the geometrization conjecture, proven by Grigori Perelman in 2005. These theorems state that every 3-manifold is canonically decomposable into submanifolds which possess a unique *geometric structure*, *i.e.* a Riemannian metric with strong homogeneity properties. There are 8 possibilities for the universal metric cover of these manifolds. One of these is *hyperbolic space*. We still do not have a satisfying understanding of hyperbolic manifolds, and this is a central open problem in the field of geometric topology.

A good way to construct a large number of 3-manifolds is to consider a knot or link complement in S^3. There are theorems which guarantee that in most cases, *i.e.* for a "generic" choice of the knot or link, the resulting manifold will be hyperbolic. On the other hand it is natural, once we build a hyperbolic manifold with a given property, to check if we can find for it a representation as a link complement.

The property which we are interested is relevant both to mathematics and physics [4], [13], and originates from the following question: *given a finite-volume hyperbolic* 3*-manifold* M*, is it the totally geodesic boundary of a finite-volume hyperbolic four manifold* $\mathcal{X}$? When this is the case, we say that M *geometrically bounds* $\mathcal{X}$ (see definition 2.17). Work of Long and Reid [10] shows that, at least in the case of compact manifolds, this property is non-trivial: a necessary condition for a closed 3-manifold to geometrically bound some compact hyperbolic 4-manifold is that its η-invariant is an integer, and there are examples of manifolds that do not satisfy this property. A result of Rohlin shows that *every* closed 3-manifold can be identified to the boundary of a compact 4-manifold, so this purely topological result does not have a geometric incarnation.

The first example of a geometrically bounding hyperbolic 3-manifold was constructed by Ratcliffe and Tschantz in [13]. The hyperbolic volume

of this example is around 200. Long and Reid built in [11] an infinite family of geometrically bounding manifolds by arithmetic methods. More recently Kolpakov, Martelli and Tschantz have provided in [7] a technique to build an infinite family of geometrically bounding 3-manifolds by pairing facets of copies of a hyperbolic 120-cell.

In this work we will concentrate on the case of noncompact manifolds. The aim is to construct the first example of a cusped hyperbolic 3-manifold which bounds geometrically a hyperbolic 4-manifold, and to represent it as a hyperbolic link complement. Our main result is the following:

Theorem 1.1. *The complement of the link in Figure 1.1 is hyperbolic. It is tessellated by eight regular ideal hyperbolic octahedra, and it geometrically bounds a hyperbolic 4-manifold $\mathcal{X}$, tesselated by two regular ideal hyperbolic 24-cells.*

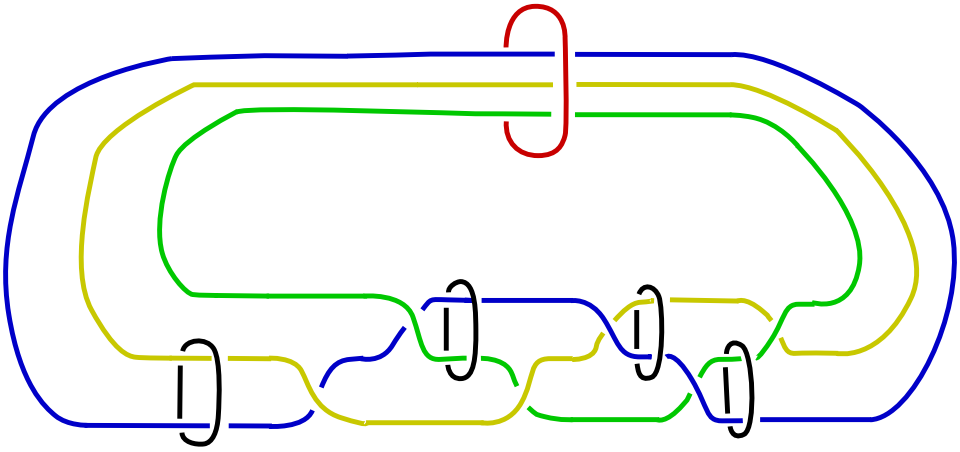

Figure 1.1: A geometrically bounding hyperbolic link complement in S^3.

We also mention that the volume of the bounding manifold of Theorem 1.1 is roughly equal to 29.311 and that, at the best of our knowledge, this is the bounding 3-manifold of smallest known volume (the smallest closed one known has volume 68.899 [7]).

Let us now outline the structure of the thesis. In chapter 2 we will recall some well known facts about hyperbolic geometry in order to establish the framework for the rest of the dissertation.

In chapter 3 we will by recall work of Costantino, Frigerio, Martelli and Petronio [2], which allows us to construct hyperbolic 3-manifolds from the data of 3-dimensional triangulations, and to represent them as the result of surgery on some components of a link in S^3.

In chapter 4 we will build the ambient 4-manifold $\mathcal{X}$ of Theorem 1.1. This will be done by pairing the facets of two regular ideal hyperbolic 24-cells. This technique dates back to work of Ratcliffe and Tschantz [14] and

has recently been exploited by Kolpakov and Martelli [6] to build the first example of hyperbolic 4 manifold with one cusp.

In chapter 5 we will describe the presentation of the boundary of $\mathcal{M}$ as a surgery over certain components of a link, and use Kirby calculus to modify it in a presentation as link complement in S^3.

In chapter 6, we will produce two examples of cusped hyperbolic 4-manifolds with empty boundary. Recall that the volume spectrum of hyperbolic 4-manifolds is the set of positive integral multiples of $v_m = 4\pi^2/3$ as shown in [14]. We say that a hyperbolic 4-manifolds has minimal volume, if its hyperbolic volume is equal to v_m. The results are the following:

Theorem 1.2. *There exists a hyperbolic 4-manifold of minimal volume v_m and two cusps.*

Theorem 1.3. *There exists a one-cusped hyperbolic 4-manifold of volume $2 \cdot v_m = 8\pi^2/3$.*

The manifold of Theorem 1.2 is, among known examples of minimal volume hyperbolic 4-manifolds, the one with the smallest number of cusps. The manifold of Theorem 1.3 is, among known one-cusped hyperbolic 4-manifolds, the one with lowest volume. It is still an open question if there exists a hyperbolic 4-manifold of minimal volume v_m with one cusp.

Chapter 2

Basics of hyperbolic geometry

We will review here some basic facts about hyperbolic geometry. For further reference on the subject, an excellent source is the book by Benedetti and Petronio [1].

It is well-known that, in every dimension $n \geq 2$, there exists a unique (up to isometry) simply connected complete Riemannian manifold with constant sectional curvature equal to -1. This manifold is called n-dimensional *hyperbolic space*, and is denoted by $\mathbb{H}^n$.

There are many different models for hyperbolic space. For our purposes, it is useful to introduce the Poincaré disk model, and the upper half-space model. Let B^n be the open unit disk in $\mathbb{R}^n$:

$$B^n = \left\{ (x_1, \ldots, x_n) \in \mathbb{R}^n \,\middle|\, \sum_{i=1}^{n} x_i^2 < 1 \right\}.$$

Definition 2.1. The Poincaré disk model for hyperbolic space is the Riemannian manifold obtained by equipping B^n with the metric tensor

$$g_x = \frac{4}{(1 - ||x||^2)^2} \cdot g_E$$

where g_E denotes the Euclidean metric tensor on $B_n \subset \mathbb{R}^n$.

Now let H^n be the upper half-space

$$H^n = \{(x_1, \ldots, x_n) |\ x_n > 0\}.$$

Definition 2.2. The upper half-space model for hyperbolic space is the Riemannian manifold obtained by equipping H^n with the metric tensor

$$g_x = \frac{1}{x_n^2} \cdot g_E$$

where $x = (x_1 \dots, x_n) \in H^n$ and g_E is the Euclidean metric tensor on $H^n \subset \mathbb{R}^n$.

We now turn our attention to the group of isometries of hyperbolic space.

Definition 2.3. Let $S_{x_0,r} \subset \mathbb{R}^n$ be the $(n-1)$-dimensional sphere of center $x_0 \in \mathbb{R}^n$ and radius $r > 0$. The *inversion* respect to $S_{x_0,r}$, denoted by $i_{x_0,r}$, is the automorphism of $\mathbb{R}^n \setminus \{x_0\}$ defined by

$$i_{x_0,r}(x) = r^2 \cdot \frac{x - x_0}{||x - x_0||^2} + x_0.$$

We can naturally extend the domain of definition of inversions to the one-point compactification $\mathbb{R}^n \cup \{\infty\} \cong S^n$ of $\mathbb{R}^n$ by requiring $S_{x_0,r}$ to exchange x_0 with the point at infinity, so that the resulting map of S^n is continuous.

Definition 2.4. Let $S^n \subset \mathbb{R}^{n+1}$ be the unit sphere, and let $C \subset S^n$ be any $(n-1)$-dimensional sphere, obtained as the intersection of S^n with an affine hyperplane $P \subset \mathbb{R}^{n+1}$. Let y be a point in $S^n \setminus C$. The stereographic projection p_y from $S^n \setminus \{y\}$ to $\mathbb{R}^n$ with pole in y maps the sphere C to some sphere $S_{x_0,r} \subset \mathbb{R}^n$. We define *inversion* respect to C, and denote I_C, the conformal automorphism of S^n which exchanges $p_y^{-1}(x_0)$ with y, and coincides with $p_y^{-1} \circ i_{x_0,r} \circ p_y$ elsewhere.

Remark 2.5. Inversions are well defined, *i.e.* do *not* depend on the choice of the pole y for the stereographic projection.

Theorem 2.6. *The group of isometries of $\mathbb{H}^n$ is isomorphic to the group $\mathrm{I}(S^{n-1})$ of automorphisms of the unit sphere $S^{n-1} \subset \mathbb{R}^n$ generated by inversions.*

Proof. (sketch) Consider the set Γ of geodesic half-rays $\gamma : [0, +\infty) \to \mathbb{H}^n$, parametrized by arc-length. We define two such half-rays to be equivalent if they asymptotically lie a bounded distance apart:

$$\gamma_1 \sim \gamma_2 \Leftrightarrow \sup\{d(\gamma_1(t), \gamma_2(t)\} < +\infty$$

where d denotes the hyperbolic distance. The boundary at infinity $\partial_\infty \mathbb{H}^n$ is defined to be the quotient of Γ under this equivalence relation.

It is possible to endow $\mathbb{H}^n \cup \partial_\infty \mathbb{H}^n$ with a topology which induces the standard topology on $\mathbb{H}^n$ and such that every isometry ϕ of $\mathbb{H}^n$ extends to a homeomorphism ϕ' of $\partial_\infty \mathbb{H}^n$ to itself. With the induced subset topology, $\partial_\infty \mathbb{H}^n$ becomes homeomorphic to the sphere S^{n-1}. This construction is best seen in Poincaré's disk model. In this case, $\mathbb{H}^n \cup \partial_\infty \mathbb{H}^n$ corresponds to the unit disk

$$D^n = \left\{ (x_1, \dots, x_n) \in \mathbb{R}^n \,\middle|\, \sum_{i=1}^{n} x_i^2 \leq 1 \right\}.$$

Every isometry of $\mathbb{H}^n$ induces an element of $\mathrm{I}(S^{n-1})$ on $\partial_\infty \mathbb{H}^n$. Conversely, every automorphism of $\partial_\infty \mathbb{H}^n$ which belongs to $\mathrm{I}(S^{n-1})$ extends to an isometry of $\mathbb{H}^n$. □

Remark 2.7. Let $C \subset S^{n-1}$ be a $(n-2)$-dimensional circle, obtained as the intersection of the unit sphere S^{n-1} with an affine hyperplane $P \subset \mathbb{R}^n$. The convex envelope of C in $\mathbb{H}^n$ is an $(n-1)$-dimensional hyperbolic subspace, and the inversion I_C corresponds to a reflection of $\mathbb{H}^n$ along such subspace. Therefore, the full isometry group of hyperbolic n-space is generated by reflections in its $(n-1)$-dimensional subspaces.

Remark 2.8. In the case of the upper half-space model, the boundary at infinity decomposes as the union

$$\partial_\infty \mathbb{H}^n = \mathbb{R}^{n-1} \cup \{\infty\},$$

where $\mathbb{R}^{n-1} = \{(x_1, \ldots, x_n) \in \mathbb{R}^n |\ x_n = 0\}$.

Since every isometry ϕ of hyperbolic space extends to a continuous map ϕ' of the closed ball $\mathbb{H}^n \cup \partial_\infty \mathbb{H}^n$, by Brower's fixed point theorem there has to be a fixed point for ϕ'. In fact, if ϕ has no fixed points in $\mathbb{H}^n$, there cannot be more than two fixed points on the boundary $\partial_\infty \mathbb{H}^n$. This allows to classify hyperbolic isometries into three families:

- *Elliptic* isometries, which have at least one fixed point in $\mathbb{H}^n$.
- *Parabolic* isometries, which have no fixed point in $\mathbb{H}^n$, and one fixed point in $\partial_\infty \mathbb{H}^n$.
- *Hyperbolic* isometries, which have no fixed point in $\mathbb{H}^n$ and two fixed points x and y in $\partial_\infty \mathbb{H}^n$.

Remark 2.9. Let ϕ be a hyperbolic isometry with fixed points x and y on $\partial_\infty \mathbb{H}^n$. The isometry ϕ acts as a translation along the geodesic from x to y.

2.1 Hyperbolic manifolds

Let M be a possibly non-compact smooth n-dimensional manifold, with $n \geq 2$ and $\partial M = \emptyset$.

Definition 2.10. A *complete hyperbolic structure* on M is the data of a discrete group Γ of isometries of $\mathbb{H}^n$, such that every $\gamma \in \Gamma$ is either parabolic or hyperbolic and such that M is diffeomorphic to $\mathbb{H}^n/\Gamma$. Two hyperbolic structures $M \cong \mathbb{H}^n/\Gamma_1$ and $M \cong \mathbb{H}^n/\Gamma_2$ on M are considered equivalent if there exists an isometry of $\mathbb{H}^n$ which conjugates Γ_1 and Γ_2.

The fact that every $\gamma \in \Gamma$ is either parabolic or hyperbolic means that the action of Γ on $\mathbb{H}^n$ has no fixed points. Discreteness of Γ is equivalent to the fact that the action is properly discontinuous, so the projection from $\mathbb{H}^n$ to $\mathbb{H}^n/\Gamma$ is a covering map. As a consequence of this fact, giving a complete hyperbolic structure to M is equivalent to endowing it with a complete Riemannian metric such that the universal metric cover is isometric to $\mathbb{H}^n$.

One might expect that such a strong property is shared by very few manifolds but, at least in dimensions two and three, this is not true. Every finite-type surface of negative Euler characteristic admits infinitely many non-equivalent hyperbolic structures of finite area. In dimension three, we have this astonishing result by Thurston [16]:

Theorem 2.11. *The interior of a compact orientable Haken 3-manifold M with nonempty boundary admits a complete hyperbolic structure of finite volume if and only if M is prime, homotopically atoroidal, and not homeomorphic to $T^2 \times I$, where T^2 is a 2-dimensional torus and I is a unit interval, or the manifold N defined below. A closed orientable Haken 3-manifold M admits a complete hyperbolic structure of finite volume if and only if it is homotopically atoroidal.*

A 3-manifold M is prime if every embedded separating two-sphere $S^2 \subset M$ bounds a ball $B^3 \subset M$. A 3-manifold M is irreducible if every embedded two-sphere $S^2 \subset M$ bounds a ball $B^3 \subset M$ or, equivalently, if it is prime and not a sphere bundle over the circle. A 3-manifold is Haken if it is irreducible and contains a properly embedded incompressible (*i.e.* π_1-injective) two-sided surface which is not a sphere. It is homotopically atoroidal if every π_1-injective map from a torus into M is homotopic into a boundary component.

The manifold N of Theorem 2.11 is a quotient of $T^2 \times I$ by the group $\mathbb{Z}/2\mathbb{Z}$, where T^2 is a 2-dimensional torus and $I = [-1, 1]$ is a closed segment. The generator of $\mathbb{Z}/2\mathbb{Z}$ acts on the first factor as a covering transformation of T^2 over the Klein bottle, and acts on the second factor by "flipping" it with the map $x \mapsto -x$.

There are many 3-manifolds which satisfy the hypotheses of Theorem 2.11. For instance any knot complement which is not a torus knot and not a satellite of another nontrivial knot admits a hyperbolic structure. All but a finite number of Dehn fillings on such a knot complement will produce a closed hyperbolic 3-manifold, as proven in [16]. In contrast to the case of surfaces, in all dimensions strictly greater than two, hyperbolic structures on a given manifold are unique, as stated by the Mostow-Prasad rigidity theorem.

2.1.1 Horospheres and cusps

Most of the hyperbolic manifolds that we will consider in this work are noncompact, so we need to introduce the notions of cusp and cusp shape.

Definition 2.12. Let p be a point in $\partial\mathbb{H}^n \cong S^{n-1}$. A *horosphere* centered at p is a connected hypersurface of $\mathbb{H}^n$ characterized by the property that it intersects orthogonally all geodesics with an endpoint at p.

We can visualize horospheres quite efficiently using the upper half-space model of hyperbolic space. Up to isometry, we can suppose $p = \infty$. Geodesics with endpoints on p become vertical lines, parametrized as $(x_1, \ldots, x_{n-1}, e^t)$. Horospheres centered at p then correspond to horizontal hyperplanes of the form $x_n = c$, for some $c > 0$. As a consequence of the expression of the metric tensor in the upper halfspace model (Definition 2.2), each horosphere is isometric to the Euclidean space $\mathbb{E}^{n-1}$.

Definition 2.13. A discrete group $H < \mathrm{Isom}(\mathbb{H}^n)$ is *parabolic* if all its nontrivial elements are parabolic isometries. Let $M \cong \mathbb{H}^n/\Gamma$ be a complete finite-volume hyperbolic n-manifold as in Definition 2.10. A *cusp* of M is a conjugacy class in Γ of a maximal parabolic subgroup $H < \Gamma$.

All the non-trivial elements of a maximal parabolic subgroup $H < \Gamma$ have a common fixed point p on the sphere $\partial\mathbb{H}^n$. H acts through isometries on any euclidean horosphere centered at p, moreover this action is free and properly discontinuous.

Definition 2.14. Let $H \subset \Gamma$ be a maximal parabolic subgroup with fixed point p. The *cusp shape* or *cusp section* of the cusp $[H] = [gHg^{-1}]$ is the homothety class of the Euclidean $(n-1)$-manifold N obtained by considering the quotient

$$N = \mathbb{E}^{n-1}/H$$

where $\mathbb{E}^{n-1}$ is a horosphere centered at p.

Each cusp $[H]$ of a hyperbolic manifold M geometrically corresponds to a submanifold $M' \subset M$ isometric to

$$N \times [0, +\infty)$$

with metric tensor in (x, t) given by

$$\frac{g_E \oplus 1}{t^2}$$

where g_E is one (suitably scaled) Euclidean metric tensor on the cusp section N.

2.1.2 Manifolds with boundary

In this section we concentrate on (possibly noncompact) manifolds with non-empty boundary. By "boundary" of a manifold, we mean the set of points of the manifold that possess open neighbourhoods isomorphic to a Euclidean halfspace, *i.e.* we do *not* consider the cusp sections of hyperbolic manifolds as boundary components.

Definition 2.15. Let M be a Riemannian manifold. A submanifold $S \subset M$ is *totally geodesic* if any geodesic in M tangent to S at some point lies entirely in S.

Definition 2.16. Let M be a (possibly noncompact) Riemannian n-manifold with non-empty boundary. M admits a complete hyperbolic structure with totally geodesic boundary if its universal metric cover is a convex set $C \subset \mathbb{H}^n$, bounded by geodesic hyperplanes in $\mathbb{H}^n$.

If a manifold M satisfies the hypothesis of Definition 2.16, its boundary components will be endowed with a hyperbolic structure. Notice that these boundary components are not necessarily compact. There is a discrete group of isometries $\Gamma < \mathrm{Isom}(\mathbb{H}^n)$ which preserves the convex subset C, so that $M \cong C/\Gamma$. Let $p \in \partial\mathbb{H}^n$ be a parabolic fixed point for the action of Γ. Without loss of generality, we can suppose $p = \infty$ in the upper-halfspace model for hyperbolic space. As mentioned previously, horospheres centered at p correspond to hyperplanes of the form $x_1 = c$, for some $c > 0$. Up to choosing c sufficiently large, the corresponding horospheres in $\mathbb{H}^n$ will intersect the convex subset C in simply connected flat $(n-1)$-manifolds, possibly with totally geodesic boundary. The cusp sections of the manifold M will be the quotients of these flat $(n-1)$-manifolds under maximal parabolic subgroups of Γ. Note that we allow the presence of closed cusp sections of M, i.e. cusps which are not bounded by components of ∂M.

Definition 2.17. Let M be a (possibly noncompact) complete finite volume hyperbolic n-manifold such that $\partial M = \emptyset$. We say that M *geometrically bounds* a complete hyperbolic $(n+1)$ manifold $\mathcal{M}$ of finite volume if:

1. $\mathcal{M}$ has only one boundary component;
2. There exists an isometry between M and $\partial\mathcal{M}$.

2.2 Link complements and Kirby calculus

In this section, we will briefly recall a series of well-known facts concerning representations of 3-manifolds. Excellent references for the subject are the books of Lickorish [9] and Rolfsen [15].

Definition 2.18. A *link* in S^3 is the data of smooth embeddings $c_1, \ldots, c_n$ of a finite number n of copies (called components) of the circle S^1 in the 3-dimensional sphere S^3, where we require the images of the embeddings to be disjoint. Two such embeddings are considered equivalent if they are obtained from each other by an isotopy of S^3, or by precomposing some of the embeddings with an orientation reversing map of S^1. A *knot* is a link with one component.

Let us consider a link L in S^3 with components $c_1, \ldots, c_n$. We can choose, canonically up to isotopy, pairwise disjoint open tubular neighborhoods U_i of the image of each component c_i. The complement of $U_1 \cup \cdots \cup U_n$ in S^3 is a compact 3-manifold with boundary which we call *exterior* of the link L and denote by M_L. The boundary of M_L consists of tori $T_1 \cup \cdots \cup T_n$, one for each component c_i, $i = 1 \ldots n$ of the link.

Definition 2.19. A *Dehn filling* on a component c_i of L is the operation of gluing a solid torus $D^2 \times S^1$ to the corresponding boundary component T_i of the manifold M_L through a homeomorphism $\phi : \partial D^2 \times S^1 \to T_i$. Up to homeomorphism, the result depends only on the isotopy class in T_i of the image of the meridian $\partial D^2 \times \{*\}$.

In order to specify a Dehn filling we need a system of coordinates for the set of essential simple closed curves on the tori T_i. A Seifert surface for a knot K in S^3 is an embedded orientable surface $F \subset S^3$ with one boundary component and such that $F \cap \mathrm{im}(K) = \partial F$. Such a surface exists for any knot K. The isotopy class of the intersection of ∂F with the torus ∂M_K is independent of the choice of the Seifert surface and determines a simple closed curve that we call *longitude* of ∂M_K. Given L, we regard each of its components as a knot in S^3, so this construction determines one longitude l_i for each component T_i of ∂M_L.

A small loop in S^3 which encircles c_i determines up to isotopy another simple closed curve on T_i that we call *meridian* and denote by m_i. Up to isotopy, we can suppose that l_i intersects m_i transversely in a single point p_i of T_i. Notice that an orientation on S^3 determines an orientation on each boundary component T_i of M_L.

Let's pick a vector v_i tangent to m_i in p_i and a vector w_i tangent to l_i in the same point, so that the ordered couple (v_i, w_i) is positively oriented with respect to the orientation on the torus T_i. The vectors v_i and w_i determine orientations for the curves m_i and l_i. Notice that once we make such a choice, we can simultaneously change the tangent vectors v_i and w_i and the orientations on the curves m_i and l_i to their opposites without affecting the condition on the compatibility of the orientations.

The homology classes of the oriented meridian and longitude form a basis of $H_1(T_i, \mathbb{Z}) \cong \mathbb{Z} \oplus \mathbb{Z}$ which, with a slight abouse of notation, we continue to denote by m_i and l_i. The homology class of every essential simple closed curve γ on T_i can therefore be expressed as $p \cdot m_i + q \cdot l_i$, where p and q are coprime integers. This determines the *slope* $p/q \in \mathbb{Q} \cup \{\infty\}$ of the curve γ. Notice that changing simultaneously the orientations of m_i and l_i does *not* affect the slope of a simple closed curve on T_i.

A consequence of this fact is that the result a Dehn filling on a component of a link is determined by the specification of a slope $s \in \mathbb{Q}$ for that given component: we glue the meridian $\partial D^2 \times \{*\}$ to the curve of slope s and extend this to a homeomorphism of the whole torus.

Definition 2.20. A *framed* link is the data of a link in S^3 and the choice of a slope (the framing) in $\mathbb{Q} \cup \{\infty\}$ for each component. A link is *partially framed* if the framing specified only on some of the components.

A framed link $F = (c_1, \dots c_n, s_1, \dots, s_n)$ specifies a closed 3-manifold M_F obtained by Dehn filling the components along the framings. In a similar way, a partially framed link specifies a manifold with a finite number of tori as boundary. Notice that we can visualize the framing of a component c_i by enlarging $\mathrm{im}(c_i)$ to an annulus $A_i \cong [-1, 1] \times S^1$ in S^3, in such a way that the boundary curves $\{-1\} \times S^1$ and $\{1\} \times S^1$ have the prescribed slope on T_i. Conversely, the choice of an annulus $[-1, 1] \times S^1$ in S^3 with the image of a component c_i as its core $\{0\} \times S^1$ determines a simple closed curve $\{1\} \times S^1$ on T_i, and therefore a framing on c_i.

Framed links are indeed a very powerful tool to represent 3-manifolds. A celebrated theorem by Lickorish and Wallace ([8], [18]) states that *every* closed orientable 3-manifold can be obtained by Dehn filling on a framed link in S^3, with all framings belonging to $\mathbb{Z}$. As an obvious consequence every orientable compact 3-manifold bounded by tori can be obtained by Dehn filling with integral framings on a partially framed link in S^3.

2.2.1 Basics of Kirby calculus

From now on we will, with a slight abuse of notation, denote the image $\mathrm{im}(L) \subset S^3$ of a link by L. Similarly, we will denote the images $\mathrm{im}(c_i)$ of its components by c_i. We will furthermore suppose that all the framings are integers.

The presentation of a 3-manifolds by surgery on a framed link is not unique. There are various moves over framed links that do not affect the homeomorphism type of the resulting manifold. Two of these are described as follows:

Definition 2.21. A *handle slide* of a framed component c_i over a framed component c_j replaces c_i with a new framed component c_i' which is built in the following way: connect the boundaries of the annuli A_i and A_j with a band $[0, 1] \times [0, 1]$ in $S^3 \setminus L$. We require two opposite sides $\{0\} \times [0, 1]$ and $\{1\} \times [0, 1]$ to be glued to A_i and A_j respectively, producing a subset F of S^3 homeomorphic to a sphere with three disjoint open disks removed. The curves c_i and c_j naturally embed in F as simple closed curves parallel to two different boundary components. The component c_i' is represented by the curve parallel parallel to the third boundary component of F, as in figure 2.1. A regular neighborhood of c_i' in F is an annulus with c_i' as core curve, and determines the framing on c_i'.

Definition 2.22. Let c_1 be an unknotted component of $L = \{c_1, \dots, c_n\}$ with framing ± 1. The curve $c_1 \subset S^3$ bounds a 2-dimensional disk $D \subset S^3$.

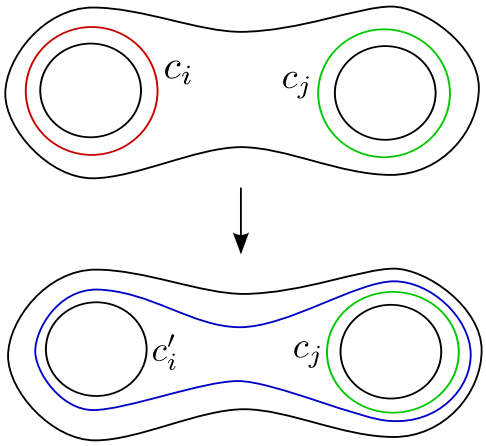

Figure 2.1: A handle slide.

Up to isotopy, we can suppose that D intersects transversely all other components of L. A regular neighborhood of $\mathrm{int}(D)$ in $S^3 \setminus c_1$ is homeomorphic to $B^2 \times [0,1]$, where B^2 is the open unit ball in the complex plane $\mathbb{C}$, and, up to isotopy, we can suppose that it intersects the other components of L in a finite amount of segments, called *strands*, of the form $\{p\} \times [0,1]$, with $p \in B^2$.

There is an automorphism ϕ of $B^2 \times [0,1]$ defined by $\phi(z,t) = (e^{\mp 2\pi t} \cdot z, t)$ which is the identity on $B^2 \times \{0,1\}$. We modify the link L to a new link L' by applying the map ϕ to $B^2 \times [0,1]$ and removing the unknotted component c_1. The conventions for the signs in the expression for ϕ is the following: there is a $+$ (resp. $-$) sign if c_1 has framing -1 (resp. $+1$).

This move changes the framings, if any are specified, on the components c_i, $i \neq 1$. Recall that a framing on c_i is specified by the choice of a small annulus A_i in S^3, with c_i as its core curve. Up to an appropriate choice of these annuli, we can suppose that they are pairwise disjoint and intersect $B^2 \times [0,1]$ in sets of the form $I \times [0,1]$, where $I \subset B^2$ is homeomorphic to a closed segment. By applying ϕ we obtain new annuli whose core curves correspond to the framed components of L', and therefore new framings on these components. This operation is called a *blow-down*. The inverse of this operation is called *blow-up*.

A blow-down is represented in Figure 2.2, in the special case where there are three strands intersecting the disk D.

Kirby ([5]) and Fenn and Rourke ([3]) prove that the moves of Definitions 2.21 and 2.22 suffice: any two framed links with integral framings representing the same manifold can be obtained from each other through isotopies and a finite number of handle slides and blow-ups/downs. We remark that Martelli [12], has exhibited a *finite* set of *local* moves that allow us to relate framed links with homeomorphic associated manifolds.

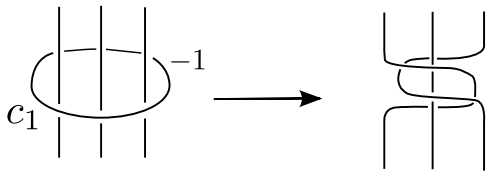

Figure 2.2: A blow-down along an unknotted component with framing -1.

Chapter 3

Hyperbolic 3-manifolds from triangulations

In this chapter we will give a brief overview of a construction contained in [2], which allows us to build a large family of hyperbolic 3-manifolds.

Consider the regular Euclidean octahedron O, which is the convex hull in $\mathbb{R}^3$ of the points $(\pm 1, 0, 0)$, $(0, \pm 1, 0)$ and $(0, 0, \pm 1)$. The octahedron O has eight 2-dimensional triangular faces, each lying in an affine plane of equation $\pm x_1 \pm x_2 \pm x_3 = 1$. Notice that these faces have a red/blue checkerboard coloring, so that each edge of O is adjacent to triangles of different colors.

Definition 3.1. The octahedron O has a realization as a hyperbolic polytope which is obtained in the following way:

1. Interpret S^2 as the boundary $\partial\mathbb{H}^3$ of hyperbolic space.
2. Consider the convex envelope in $\mathbb{H}^3$ of the vertices $v_1, \ldots, v_6$ of O.

The convex subset of $\mathbb{H}^3$ that we obtain is the *regular ideal hyperbolic* octahedron $\mathcal{O}$.

The eight vertices of O correspond to cusps of $\mathcal{O}$, and the checkerboard coloring of the faces of O induces one on $\mathcal{O}$.

Definition 3.2. The *Minsky block* B is the orientable cusped hyperbolic 3-manifold obtained from two copies $\mathcal{O}_1$ and $\mathcal{O}_2$ of the regular ideal hyperbolic octahedron $\mathcal{O}$ by gluing the *red* boundary faces of $\mathcal{O}_1$ to the corresponding red boundary faces of $\mathcal{O}_2$ via the map induced by the identity on the faces of $\mathcal{O}$.

Each of the four boundary components of B is obtained by gluing two copies of a hyperbolic ideal triangle along the boundary via the identity map, therefore it is a sphere with three punctures. Moreover B has six cusps which all have the same shape, namely a flat annulus of length two and width one (up to homothety).

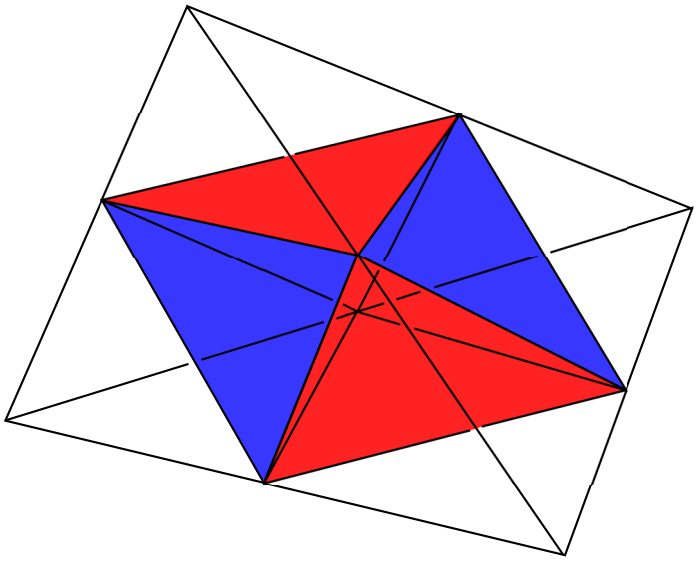

Figure 3.1: Truncating a tetrahedron produces an octahedron.

There is a combinatorial equivalence between certain strata of the octahedron O and those of a regular euclidean tetrahedron T. To see this, notice that it is possible to build an octahedron from a tetrahedron T by truncating T and enlarging the truncated regions until they become tangent at the midpoints of the edges. We can also recover the checkerboard coloring, by declaring the truncation faces to be red, and those contained in the faces of T to be blue. As shown in Figure 3.1, the following correspondences hold:

1. $\{\text{Vertices of } T\} \leftrightarrow \{\text{Red faces of } O\}$;
2. $\{\text{Edges of } T\} \leftrightarrow \{\text{Vertices of } O\}$;
3. $\{\text{Faces of } T\} \leftrightarrow \{\text{Blue faces of } O\}$.

Since the Minsky block B is the double along the red faces of a regular ideal hyperbolic octahedron $\mathcal{O}$, the correspondences above induce the following correspondences between strata of B and T:

1. $\{\text{Edges of } T\} \leftrightarrow \{\text{Cusps of } B\}$.
2. $\{\text{Faces of } T\} \leftrightarrow \{\text{Boundary components of } B\}$;

Proposition 3.3. *There is an isomorphism ϕ between the symmetry group of the tetrahedron T and the group of orientation-preserving isometries of the block B.*

Proof. Every isometry of B preserves its tessellation into regular ideal hyperbolic octahedra $\mathcal{O}_1$ and $\mathcal{O}_2$. There is an orientation-reversing involution

j of B which exchanges the two ideal octahedra $\mathcal{O}_1$ and $\mathcal{O}_2$, induced by the identity map on $\mathcal{O}$. Every orientation-preserving isometry of B can be brought, composing it with j if necessary, to fix the octahedra $\mathcal{O}_i$, $i = 1, 2$. This induces a symmetry of the regular octahedron O which preserves the red/blue coloring of its triangular faces. Such a symmetry of O is induced by a unique symmetry of the tetrahedron T. This construction defines the map ϕ, which is easily seen to be an isomorphism. □

A consequence of the correspondences above is that a set of simplicial pairings between the facets of n copies of the tetrahedron T encodes a set of gluings between the boundary components of n copies of the Minsky block B, allowing us to produce a hyperbolic 3-manifold from the simple data of a 3-dimensional triangulation.

Definition 3.4. A 3-*dimensional triangulation* is a pair

$$(\{\Delta_i\}_{i=1}^{n}, \{g_j\}_{j=1}^{2n})$$

where n is a positive natural number, the Δ_i's are copies of the standard tetrahedron, and the g_j's are a complete set of simplicial pairings between the $4n$ faces of the Δ_i's. The triangulation is *orientable* if it is possible to choose an orientation for each tetrahedron Δ_i so that all pairing maps between the faces are orientation-reversing.

Definition 3.5. Let $\mathcal{T} = (\{\Delta_i\}_{i=1}^{n}, \{g_j\}_{j=1}^{2n})$ be an orientable triangulation as in Definiton 3.4. We associate to each Δ_i a copy B_i of the Minsky block B. A face pairing g_j between triangular faces F and G of tetrahedra Δ_i and Δ_j determines a *unique* orientation-reversing isometry ϕ_j between the boundary components of B_i and B_j corresponding to F and G, by the condition that their cusps are paired according to the pairing of the edges of $\mathcal{T}$. We denote the manifold obtained by pairing the boundary components of the blocks $B_1, \ldots, B_n$ via the isometries $\phi_1, \ldots, \phi_{2n}$ by $M_{\mathcal{T}}$.

Proposition 3.6. *The manifold $M_{\mathcal{T}}$ constructed from a triangulation $\mathcal{T}$ as in Definition 3.5 is an orientable cusped hyperbolic manifold of finite volume.*

Proof. The manifold $M_{\mathcal{T}}$ is clearly a noncompact manifold with empty boundary. Let us view it as the result of a gluing of regular ideal hyperbolic octahedra. We have a hyperbolic structure on the complement of the 1-skeleton and we need to check that it extends around the edges. Following chapter 4 of [17], this is equivalent to showing that the horoball sections of the vertex links of the blocks B_i, which are flat annuli of length two and width one, glue together to give a closed flat surface. The result of the glueings is to join these annuli along their boundary components, producing a flat torus. The volume of $M_{\mathcal{T}}$ is $2n \cdot v_{\mathcal{O}}$, where n is the number of tetrahedra of the triangulation and $v_{\mathcal{O}} \approx 3.664$ is the volume of a regular ideal hyperbolic octahedron. □

Remark 3.7. The cusps of the manifold $M_{\mathcal{T}}$ are in one-to-one correspondence with the edges of the triangulation $\mathcal{T}$, and that the number of annuli which are glued together to build a cusp is equal to the valence of the corresponding edge.

3.1 Hyperbolic relative handlebodies

In this section we will discuss the topological structure of the hyperbolic manifolds constructed from 3-dimensional triangulations.

Definition 3.8. A *relative handlebody* (H, Γ) is an orientable handlebody H with a finite sysytem Γ of disjoint nontrivial loops in its boundary. A *hyperbolic structure* on (H, Γ) is a finite-volume complete hyperbolic structure on the manifold $H \setminus \Gamma$, such that the boundary $\partial H \setminus \Gamma$ is totally geodesic.

Given an orientable 3-dimensional triangulation $\mathcal{T} = (\{\Delta_i\}_{i=1}^n, \{g_j\}_{j=1}^{2n})$ as in Definition 3.4, there is a canonical way to associate to $\mathcal{T}$ a relative handlebody $H_{\mathcal{T}}$. We begin by considering the support $|\mathcal{T}|$ of the trianguation, which is the topological space obtained by glueing the tetrahedra of $\mathcal{T}$ according to the face pairings, with its CW-complex structure. Then we remove a regular open neighborhood of its 1-skeleton.

We call H the resulting space, which is a handlebody since it has a handle decomposition obtained from a collection of disjoint balls (corresponding to the tetrahedra of T) by attaching 1-handles according to the face pairings. The genus of the handlebody is $n + 1$, where n is the number of tetrahedra of $\mathcal{T}$.

To each edge e of $\mathcal{T}$ we associate a simple closed loop in ∂H, corresponding to a simple closed curve in $|\mathcal{T}|$ which encircles e. These loops form a system Γ of curves in ∂H, and we define the realtive handlebody $H_{\mathcal{T}}$ as the pair (H, Γ).

With a slight abuse of notation, we denote by $H \setminus \Gamma$ the complement in H of the curves of Γ. A vital observation is that we can endow $H \setminus \Gamma$ with a hyperbolic structure. To do so, we associate to every tetrahedron Δ_i of $\mathcal{T}$ a colored regular ideal hyperbolic octahedron $\mathcal{O}_i$ as in Figure 3.1 and glue the blue faces of the octahedra $\mathcal{O}_i$, $i = 1, \ldots, n$, together according to the face pairings of $\mathcal{T}$.

The red faces will glue together along their edges to give the totally geodesic boundary of $H \setminus \Gamma$. Each $\gamma \in \Gamma$ corresponds to an edge e of $\mathcal{T}$, and to each such edge corresponds an equivalence class of ideal vertices of the octahedra. These vertices are glued together to produce the cusp associated to γ. The shape of the cusp associated to the edge e is that of a flat annulus obtained by identyfing sides of $\{0\} \times [0, 1]$ and $\{n\} \times [0, 1]$ of a rectangle $[0, n] \times [0, 1]$, where n is the valence of e.

Proposition 3.9. *Given an orientable 3-dimensional triangulation $\mathcal{T}$, the manifold $M_{\mathcal{T}}$ is the double of $H \setminus \Gamma$ along its boundary, where $H_{\mathcal{T}} = (H, \Gamma)$ is the hyperbolic relative handlebody associated to $\mathcal{T}$.*

Proof. The manifold $H \setminus \Gamma$ is built by glueing together the blue faces of a set of regular ideal hyperbolic octahedra. Its boundary is tessellated in a loose sense by the red faces of the resulting complex. The manifold $M_{\mathcal{T}}$ is built by glueing together the boundary components of copies of the block B.

Mirroring a regular ideal hyperbolic octahedron $\mathcal{O}$ along its red faces produces the block B. The boundary components of B are the doubles of the blue faces of $\mathcal{O}$ along the ideal edges. The glueing of these boundary components is obtained by doubling in the obvious way the glueing of the blue faces of $\mathcal{O}$, since both are determined by the face pairings of the triangulation $\mathcal{T}$ and the orientation-reversing condition. □

3.2 Presentations as a surgery along partially framed links

We wish to construct a presentation of any manifold $M_{\mathcal{T}}$ associated to an orientable 3-dimensional triangulation $\mathcal{T} = (\{\Delta_i\}_{i=1}^n, \{g_j\}_{j=1}^{2n})$, as a surgery over a partially framed link. As a consequence of Proposition 3.9, the manifold $M_{\mathcal{T}}$ is the complement of a link in a manifold N obtained by mirroring an orientable handlebody H along its boundary. As mentioned before, the handlebody H consists of n 0-handles (one for each tetrahedron of T), and $2n$ 1-handles (one for each g_j). The handlebody H has genus $n+1$, therefore the manifold N is a connected sum of $n+1$ copies of $S^2 \times S^1$. The boundary of H corresponds to an embedded surface S of genus $n+1$ in N.

The manifold N has a presentation as surgery on the trivial $n+1$-component link, with all framings equal to zero. This can be easily seen by noticing that the Dehn filling on the unknot with zero framing produces $S^2 \times S^1$ as a result.

We can visualize the handlebody H and the surface corresponding to ∂H in this presentation. To do so, we embed the handlebody H in $S^3 = \mathbb{R}^3 \cup \{\infty\}$, starting from a disjoint union of balls $B_1, \ldots, B_n$ in $\mathbb{R}^3$ and connecting them with 1-handles according to the face pairings. We pick a collection of $n+1$ one-handles in such a way that removing them from H yields topologically a 3-dimensional ball. We encircle these handles with small zero-framed components. The resulting trivial $n+1$ component link, with zero framings on every component, is a presentation of N as mentioned previously.

Now we have to describe which curves to remove from N to obtain the cusps of $M_{\mathcal{T}}$. Notice that these curves can be represented as a system $A = (a_1, \ldots, a_m)$ of disjoint nontrivial loops on the surface ∂H as follows. ∂H

has an obvious decomposition into a union of n four-holed spheres $S_1, \ldots, S_n$ induced by the decomposition of H as a union of handles.

Every 4-holed sphere S_i corresponds to a tetrahedron of Δ_i of $\mathcal{T}$, and every boundary component of S_i corresponds to a face of Δ_i. Two of these 4-holed sphere S_i and S_j share a boundary component if there is a face pairing g_k between the correponding faces of Δ_i and Δ_j.

The face pairings of $g_1, \ldots, g_{2n}$ define a way to pick in each S_i a complete system of disjoint arcs connecting the boundary components, each arc corresponding to an edge of Δ_i, in such a way that the endpoints of these arcs join along the intersections $S_i \cap S_j$ (see Figure 3.2). Different choices for these systems of arcs in ∂H differ by Dehn twists along the curves $S_i \cap S_j$. Adding the loops of A to the presentation of the manifold N produces a presentation of the manifold $M_{\mathcal{T}}$ as a partially framed link.

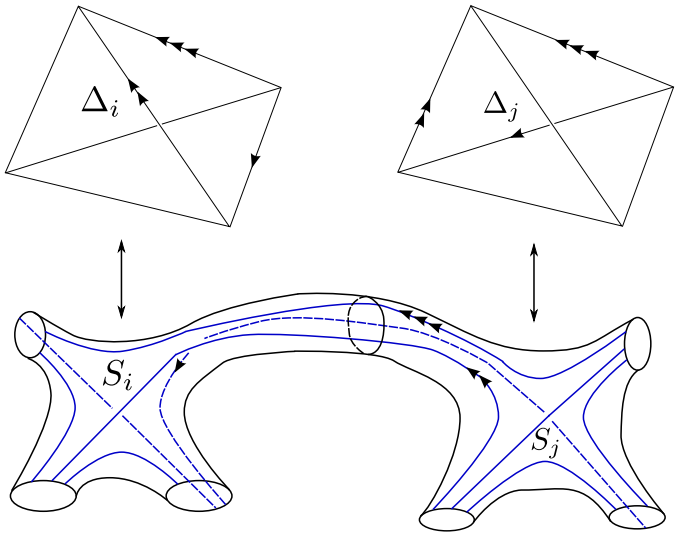

Figure 3.2: A face pairing between faces of tetrahedra Δ_i and Δ_j defines a way to join the arcs (colored in blue) in the 4-holed spheres S_i and S_j to produce a set of loops in ∂H.

Remark 3.10. In the construction of this presentation we have made a number of choices: the embedding of the handlebody H in $\mathbb{R}^3$, the choice of the one-handles around which we place the framed components of the link and the number of "twists" along the curves $S_i \cap S_j$ we use to connect the arcs to build A. All these different choices are related by a sequence of handle slides along zero-framed components (see [2] and [12]).

Example 3.11. Consider the orientable triangulation $\mathcal{T}$ obtained by mirroring a tetrahedron T in its boundary. Formally, we take two copies T_1 and T_2 of T, with opposite orientations, and glue them together along their

boundary via the identity map. A presentation of the manifold $M_{\mathcal{T}}$ associated to this triangulation is given in Figure 3.3.

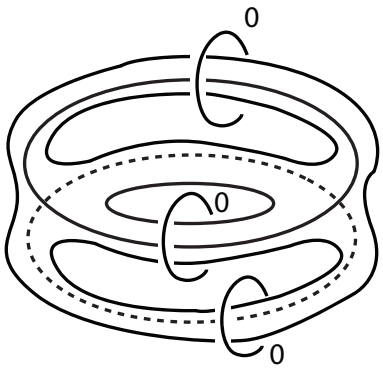

Figure 3.3: Presentation as a partially framed link of the manifold $M_{\mathcal{T}}$, where $\mathcal{T}$ is the triangulation obtained by mirroring a tetrahedron in its boundary.

Example 3.12. Let $\mathcal{T}$ be the orientable triangulation obtained from a tetrahedron T through the following process: pick a pair of opposite edges a and b, such that a separates face A_1 and A_2 and b separates faces B_1 and B_2. Identify the faces A_1 and A_2 by the unique orientation reversing map which fixes their common edge, i.e. by "folding" along a, and do the same for B_1 and B_2, as in Figure 3.4.

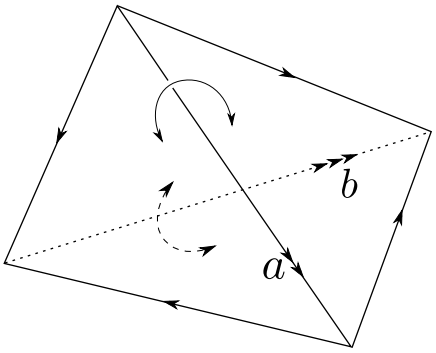

Figure 3.4: Triangulation associated to a small boundary component.

The resulting manifold $M_{\mathcal{T}}$ has three cusps, and a presentation as partially framed link is given in Figure 3.5.

As we will see in the next chapters, it is possible to modify the presentations as a partially framed links of the manifold $M_{\mathcal{T}}$ constructed from a

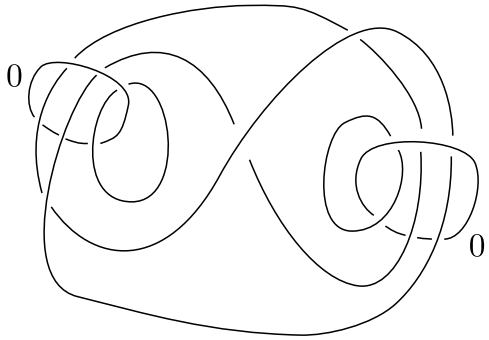

Figure 3.5: Presentation as a partially framed link of the manifold $M_{\mathcal{T}}$, where $\mathcal{T}$ is the triangulation defined in Example 3.12

triangulation $\mathcal{T}$ using isotopies, handle slides and blow-ups/downs. If we can get rid of the framed components, the result is a presentation of M_T as a link complement in S^3. As shown in [6], in the case of Example 3.11, the manifold $M_{\mathcal{T}}$ is the exterior of the minimally twisted 6-chain link, shown in Figure 3.6.

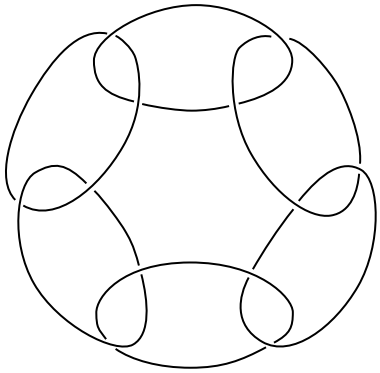

Figure 3.6: The minimally twisted 6-chain link.

Chapter 4

The ambient 4-manifold

In this chapter, we will construct the non-compact complete finite-volume hyperbolic 4-manifold $\mathcal{X}$ of Theorem 1.1. We begin by introducing the 4-dimensional polytope which tessellates it.

4.1 The 24-cell

The 24-cell C is the only regular polytope in any dimension $n \geq 3$ which is self-dual and not a simplex. It is defined as the convex hull in $\mathbb{R}^4$ of the set of points obtained by permuting the coordinates of

$$(\pm 1, \pm 1, 0, 0).$$

It has 24 vertices, 96 edges, 96 faces of dimension 2 and 24 facets of dimension 3 which lie in the affine hyperplanes of equations

$$x_i = \pm 1, \quad \pm x_1 \pm x_2 \pm x_3 \pm x_4 = 2.$$

The dual polytope C^* is the convex hull

$$C^* = \mathrm{Conv}\{\mathcal{R}, \mathcal{B}, \mathcal{G}\}$$

where $\mathcal{G}$ is the set of 8 points obtained by permuting the coordinates of

$$(\pm 1, 0, 0, 0)$$

and $\mathcal{R} \cup \mathcal{B}$ is the set of 16 points of the form

$$\left(\pm\frac{1}{2}, \pm\frac{1}{2}, \pm\frac{1}{2}, \pm\frac{1}{2}\right),$$

with $\mathcal{R}$ (resp. $\mathcal{B}$) being the set of 8 points with an even (resp. odd) number of minus signs in their entries. The facets of C are regular octahedra in canonical one-to-one correspondence with the vertices of C^*, and are colored

accordingly in red, green and blue. This coloring is natural; every symmetry of the 24-cell C preserves the partition of the vertices of C^* into the sets $\mathcal{R}, \mathcal{B}, \mathcal{G}$, and every permutation of $\{\mathcal{R}, \mathcal{G}, \mathcal{B}\}$ is realized by a symmetry of C. The vertex figure is a cube, in accordance with self-duality. Notice furthermore that the convex envelope of $\mathcal{R} \cup \mathcal{B}$ is a hypercube, while the convex envelope of $\mathcal{G}$ is a 16-cell.

Definition 4.1. The 24-cell has a hyperbolic ideal realization, analogous to the one described in Chapter 3 for the case of the octahedron, which we call *hyperbolic ideal* 24*-cell* and denote by $\mathcal{C}$. It is obtained in the following way:

1. Normalize the coordinates of the vertices $v_1, \ldots, v_{24}$ of C so that the lie on the unit sphere S^3.
2. Interpret S^3 as the boundary $\partial\mathbb{H}^4$ of hyperbolic space.
3. Consider the convex envelope in $\mathbb{H}^4$ of the points $v_1, \ldots, v_{24}$.

The facets of $\mathcal{C}$ are regular ideal hyperbolic octahedra. The vertex figure of the hyperbolic 24-cell is a euclidean cube, therefore all dihedral angles between facets are equal to $\pi/2$, which is a submultiple of 2π. The 24-cell is the only regular ideal hyperbolic 4-dimensional polytope which has this property. This allows us to glue isometrically along their facets a finite number copies of the ideal 24-cell so that the local geometric structures on each cell piece together to give a global hyperbolic structure on the resulting non-compact manifold (see [14] and [6] for further applications of this technique).

4.2 Mirroring the 24-cell

We begin the construction of the hyperbolic 4-manifold $\mathcal{X}$ by mirroring a 24-cell along its green facets.

Definition 4.2. The *mirrored* 24*-cell* $\mathcal{S}$ is the space obtained from two copies $\mathcal{C}_1$ and $\mathcal{C}_2$ of the regular ideal hyperbolic 24-cell $\mathcal{C}$ with opposite orientations, by gluing each green facet of $\mathcal{C}_1$ to the corresponding green facet of $\mathcal{C}_2$ via the map induced by the identity on $\mathcal{C}$.

Proposition 4.3. *The mirrored* 24*-cell* $\mathcal{S}$ *is a non-compact* 4*-dimensional manifold with boundary. The boundary* $\partial\mathcal{S}$ *decomposes into* 16 *strata of dimension* 3*, each isomorphic to the Minky block* B *of Definition 3.2. These boundary strata intersect at* 32 *strata of dimension* 2*, each isomorphic to a sphere with three punctures, with dihedral angle* $\pi/2$*.*

Proof. Each boundary 3-stratum is obtained by doubling a red or a blue octahedral facet of $\mathcal{C}$ along the triangular faces that separate it from a green

octahedral facet. Up to an appropriate choice of the coloring, this is exactly the construction of Definition 3.2. Each boundary 2-stratum is built by mirroring in its boundary edges a triangular 2-stratum of $\mathcal{C}$ which separates a red octahedron from a blue one, producing a thrice-punctured sphere. $\square$

The cusp section of the manifold $\mathcal{S}$ is pictured in Figure 4.1. It is obtained by mirroring the cusp section of the 24-cell, which is a Euclidean cube, along a pair of opposite faces (corresponding to the green facets of $\mathcal{C}$). The result is $Q \times S^1$, where Q is a flat square with sides of length one, and the S^1 factor has length two. The boundary 3-strata naturally correspond to sets of the form $I \times S^1$, where I is a side of Q and the intersection of any two of these sets in a common edge has indeed angle $\pi/2$.

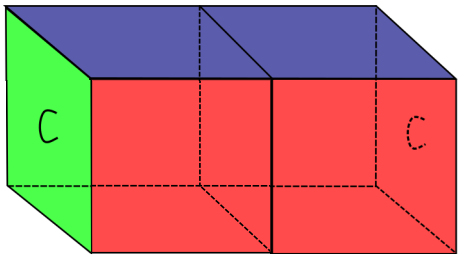

Figure 4.1: A fundamental domain for the cusp section of the mirrored 24-cell. The opposite faces of each cube share the same colour, and the green faces are identified in pairs.

There is a natural correpondence between certain strata of the mirrored 24-cell $\mathcal{S}$ and of the 24-cell $\mathcal{C}$, described as follows:

1. $\{\text{Cusps of } \mathcal{S}\} \leftrightarrow \{\text{Vertices of } \mathcal{C}\}$
2. $\{\text{Red and blue 3-strata of } \mathcal{S}\} \leftrightarrow \{\text{Red and blue facets of } \mathcal{C}\}$
3. $\{\text{2-strata of } \mathcal{S}\} \leftrightarrow \{\text{red/blue 2-stratum face of } \mathcal{C}\}$

   By red/blue 2-stratum we mean a 2-dimensional face of $\mathcal{C}$ which bounds a red facet on one side and a blue facet on the other.

The correspondence just mentioned allows us label the strata of $\mathcal{S}$ in the following way:

1. We label each cusp of $\mathcal{S}$ with the corresponding vertex of the 24-cell $\mathcal{C}$, which is given by a permutation of the 4-uple $(\pm 1, \pm 1, 0, 0)$. For brevity we write $\pm$ instead of ± 1. Notice that there always have to be two 0 entries.
2. Each red or blue facet of the 24-cell lies in an affine hyperplane of equations
$$\pm x_1 \pm x_2 \pm x_3 \pm x_4 = 2$$

and we label the corresponding 3-stratum of $\mathcal{S}$ by the 4-uple of $+,-$ signs in this equation. The red/blue coloring is again determined by the parity of the number of minus signs.

3. A red and a blue facet of $\mathcal{C}$ are adjacent along a 2-stratum if and only if their labels differ by the choice of one sign. Replacing this sign by a 0, we see that the red/blue 2-strata of $\mathcal{C}$ and the correponding 2-strata of $\mathcal{S}$ are naturally labeled by 4-uples of $+,-,0$ symbols, with one 0 entry. For example, the 2-stratum which is adjacent to the 3-strata with labels $(+,+,+,+)$ and $(+,+,+,-)$ is labeled $(+,+,+,0)$.

Notice that a 3-stratum of $\mathcal{S}$ bounds a certain cusp if and only the non-zero entries in the labeling of the cusp coincide with the corresponding $+,-$ entries in the labeling of the 3-stratum.

There is a group G of affine transformations acting on the 24-cell and preserving the set of the green facets. It is generated by the reflections in the hyperplanes $\{x_i = 0\}$ and the permutations of the coordinates, and is isomorphic to a semi-direct product of $(\mathbb{Z}/2\mathbb{Z})^4$ with $\mathfrak{S}_4$. As a consequence of the correpondence between strata mentioned above, it acts also on the mirrored 24-cell $\mathcal{S}$, and we can use it to pair the boundary 3-strata.

4.3 Face pairings of the boundary 3-strata

As explained in Proposition 4.3, the 2-strata of the mirrored 24-cell $\mathcal{S}$ lie at the intersection of a red and a blue 3-stratum, and the dihedral angle at the intersection is equal to $\pi/2$. As a consequence of this fact, *any* pairing on the blue 3-strata of $\mathcal{S}$ "kills" all the 2-strata, producing a hyperbolic manifold with disjoint totally geodesic boundary components, tessellated by the red 3-strata of $\mathcal{S}$.

Definition 4.4. We denote by $\mathcal{R}$ the manifold obtained from the mirrored 24-cell $\mathcal{S} = \mathcal{C}_1 \cup \mathcal{C}_2$ by pairing its blue 3-strata in the following way:

1. $\pm(+,+,-,+)$ in $\mathcal{C}_1$ (resp. $\mathcal{C}_2$) is paired with $\pm(+,+,+,-)$ in $\mathcal{C}_1$ (resp. $\mathcal{C}_2$) via the map
$$F(x,y,z,w) = (x,y,w,z).$$

2. $\pm(+,-,+,+)$ in $\mathcal{C}_1$ (resp. $\mathcal{C}_2$) is paired with $\pm(-,+,+,+)$ in $\mathcal{C}_1$ (resp. $\mathcal{C}_2$) via the map
$$G(x,y,z,w) = (y,x,z,w).$$

Proposition 4.5. *The manifold $\mathcal{R}$ of Definition 4.4 is an orientable hyperbolic non-compact 4-manifold with totally geodesic boundary. It has ten cusps whose sections fall into three homothety classes: there are four* small *cusps, two* medium *cusps and four* large *cusps, as defined below.*

Proof. The pairing maps are simply permutation of two coordinates. Since they are orientation reversing, $\mathcal{R}$ is an orientable 4-manifold with boundary. To check that it has a complete hyperbolic structure induced from that of $\mathcal{S}$, we need to check that the cusp sections of $\mathcal{S}$ glue together into Euclidean manifolds to produce the cusp sections of $\mathcal{R}$.

For our purposes, it is convenient to have a graphical representation of the cusp sections of the mirrored 24-cell $\mathcal{S}$. Consider Figure 4.1. Notice that each cusp of $\mathcal{S}$ is bounded by four 3-strata, two red and two blue. A red and a blue 3-stratum intesect orthogonally in a 2-stratum. By taking a vertical section of parallelepiped of Figure 4.1, we obtain a planar representation where the cusp corresponds to a square, the boundary 3-strata correspond to the sides of such square, and the 2-strata correspond to the vertices as in Figure 4.2. The face pairings will induce identifications of the blue edges of the different squares, and we can describe the cusp shapes of $\mathcal{R}$ by taking the product of the resulting flat surface with a circumference S^1 of length two.

1. The four cusps labeled $\pm(+,+,0,0)$ and $\pm(0,0,+,+)$ are fixed by the face-pairing maps. The opposite blue faces of the corresponding squares are identified by the pairing maps to produce a flat cylinder C_1 of width and length equal to one. The cusp shape is a product $C_1 \times S^1$. We call these the *small* cusps of the manifold $\mathcal{R}$.

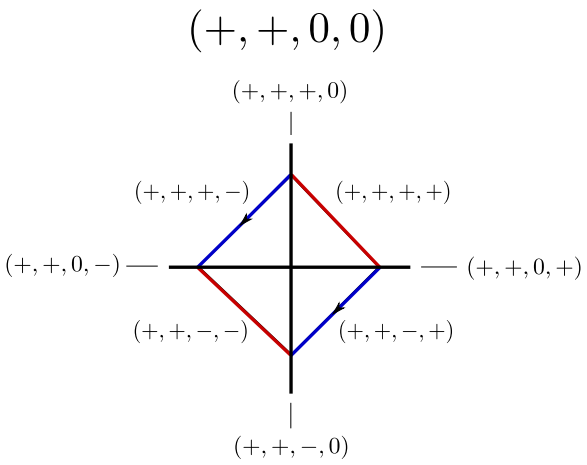

Figure 4.2: Example of planar representation of a cusp section of the mirrored 24-cell for the small cusp labeled $(+,+,0,0)$. Arrows show the pairings between the blue faces induced by the map F.

2. The cusp $(+,-,0,0)$ is paired to $(-,+,0,0)$ by G, and in a similar way $(0,0,+,-)$ is paired to $(0,0,-,+)$ by F. The identifications between the first two cusps are represented in the Figure 4.3. We call these two

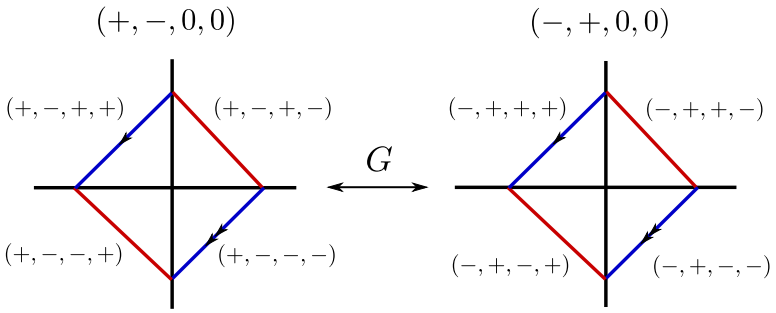

Figure 4.3: Face pairings for the medium cusp obtained by pairing $(+,-,0,0)$ to $(-,+,0,0)$ via the map G.

the *medium* cusps. The cusp shape is a product $C_2 \times S^1$, where C_2 is a cylinder of width one and length two.

3. The remaining sixteen cusps of the mirrored 24-cell are identified in four groups of four. In all these four cases, the pairings between the blue boundary components produce the same flat manifold, and one example is shown in Figure 4.4. We call these cusps *large*. The cusp shape is a product $C_3 \times S^1$, where C_3 is a cylinder of width one and length four.

□

Proposition 4.6. *The manifold $\mathcal{R}$ of Definition 4.4 has five disjoint totally geodesic boundary components which fall into two isometry classes: there are four* small *boundary components and one* large *boundary component.*

Proof. The pairings between the blue 3-strata of $\mathcal{S}$ induce identifications between the 2-dimensional strata of $\mathcal{S}$, and define therefore glueings of the red 3-strata of $\mathcal{S}$, which are copies of the Minsky block B of Definition 3.2, along their boundary components. The resulting manifolds form the totally geodesic boundary of $\mathcal{R}$, and their topology is encoded by triangulations as explained in Chapter 3.

We begin by considering the 3-strata of the mirrored 24-cell labeled $\pm(+,+,+,+)$ and $\pm(+,+,-,-)$. For each such 3-stratum, it is easy to check that the four boundary 2-strata are identified in pairs. The resulting 3-manifolds are all isometric, and are obtained from the triangulation $\mathcal{T}$ with one tetrahedron of example 3.12. We call these the *small* boundary components of the manifold $\mathcal{R}$. Let us take a look at the case of the component labeled $(+,+,+,+)$. Its four boundary components are labeled $(+,+,+,0)$, $(+,+,0,+)$, $(+,0,+,+)$ and $(0,+,+,+)$. The pairings are shown below in Figure 4.5, together with their behaviour on the cusps.

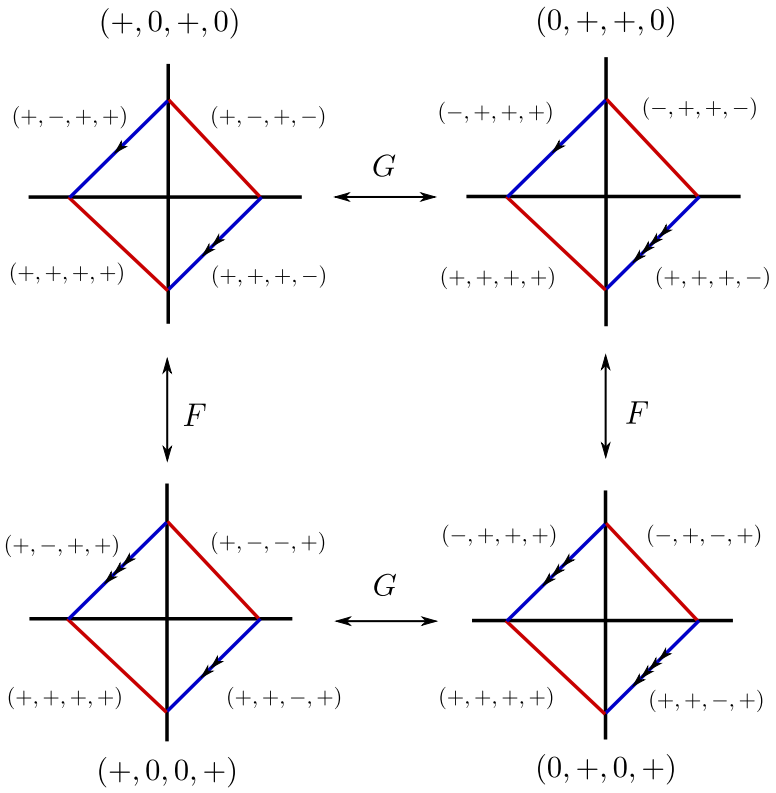

Figure 4.4: Face pairings for the large cusps.

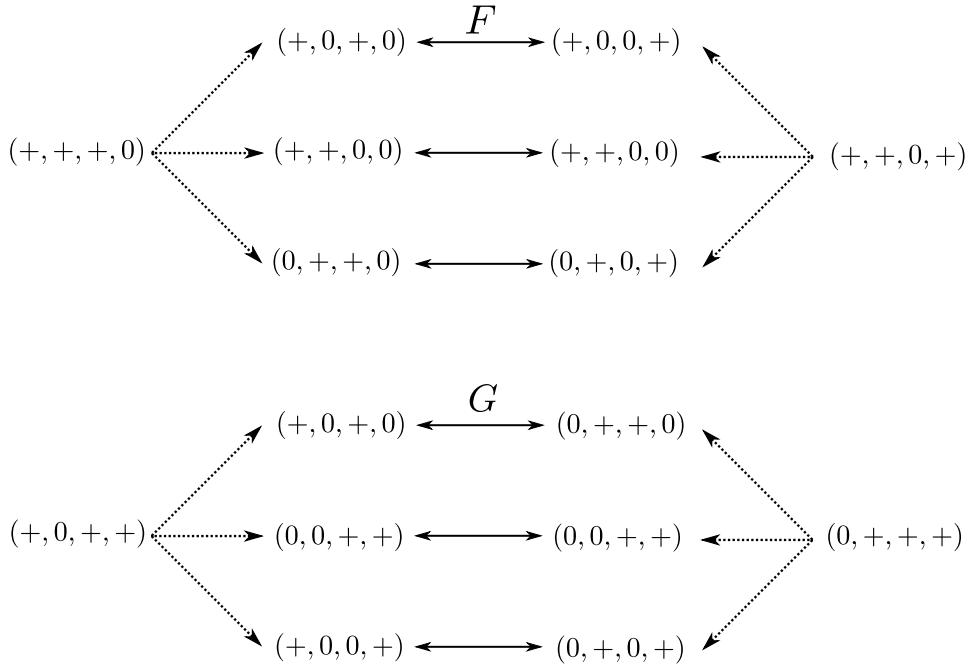

Figure 4.5: Face pairings for the boundary component $(+,+,+,+)$. Dotted lines indicate adjacencies between the boundary 2-strata and the cusps of $\mathcal{S}$.

The small boundary components have three cusps each. Two of them correspond to boundary components of a small cusp of $\mathcal{R}$, and one corresponds to a boundary component of a large cusp of $\mathcal{R}$.

There is another *large* boundary component M, obtained by glueing together the four strata labeled $\pm(+,-,+,-)$ and $\pm(+,-,-,+)$. The glueings are shown in Figure 4.6.

We have to determine how the faces are glued together, and this depends on the behaviour of the pairings on the cusps. To do so, we represent each boundary 3-stratum $\mathcal{B}_i$ with a copy $\mathcal{T}_i$ of the tetrahedron. Recall that the faces of $\mathcal{T}_i$ are in one-to-one correspondence with the boundary 2-strata of $\mathcal{B}_i$. We assign to the faces of each tetrahedron a number $n \in \{1,2,3,4\}$, with the rule that to a face is assigned the number n if the label of corresponding boundary 2-stratum has a zero in the nth entry. In each tetrahedron, every face is assigned a different number, and each edge is identified by the couple $\{i,j\}$ of integers assigned to its two adjacent faces.

Notice that all face pairings identify faces of different tetrahedra $\mathcal{T}_i$ and $\mathcal{T}_j$ in a way which *preserves* their numbering. The map F identifies faces numbered with $n \in \{1,2\}$, while G identifies faces numbered with $n \in \{3,4\}$. Furthermore the map F (resp. G) identifies the edges labeled $\{1,2\}$ (resp. $\{3,4\}$), and there is a unique way to do so in an orientation reversing way.

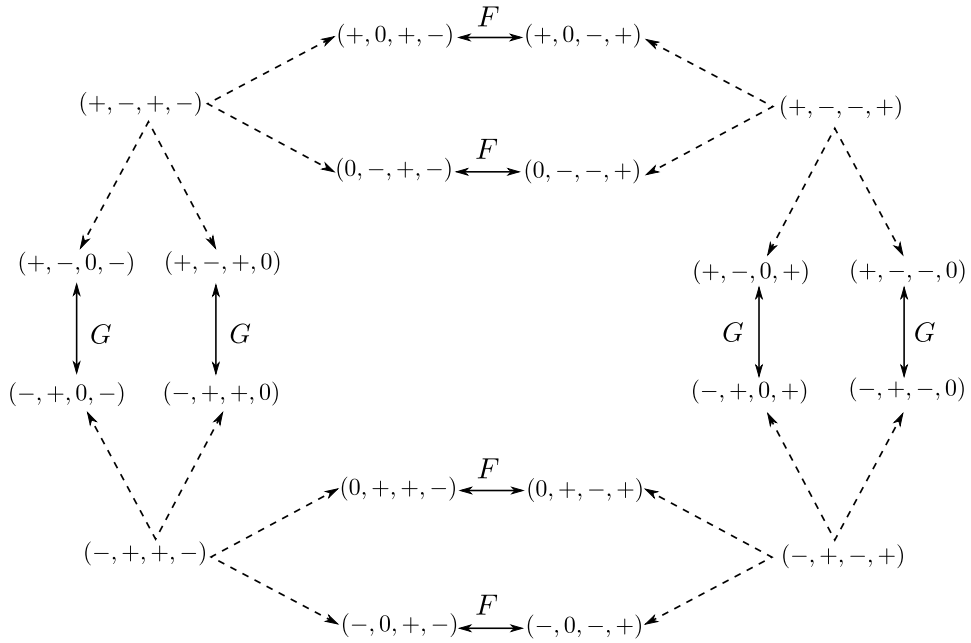

Figure 4.6: Face pairings for the large boundary component. Dashed lines indicate adjacencies between boundary 3-strata and their boundary 2-strata. The arrows labeled F and G show the face pairings between the 2-strata.

The resulting triangulation is represented in Figure 4.7.

□

Remark 4.7. The volume of the large boundary component M of the manifold $\mathcal{R}$ is $8 \cdot v_{\mathcal{O}} \approx 29.311$, where $v_{\mathcal{O}}$ is the volume of the regular ideal hyperbolic octahedron.

Remark 4.8. The large boundary component M of the manifold $\mathcal{R}$ has eight cusps, four of which come from boundary components of large cusps of $\mathcal{R}$. They have the cusp shape of a torus obtained by identifying opposite sides of a 2×4 rectangle. We call these the *large* cusps of M. The other four come from boundary components of the medium cusps of $\mathcal{R}$, and they correspond to the edges of the tetrahedra labeled $\{1, 2\}$ and $\{3, 4\}$. Their shape is that of a torus obtained by identifying opposite sides of a square of sidelength two. These are the *small* cusps of M.

Theorem 4.9. *The large boundary component M of the manifold $\mathcal{R}$ geometrically bounds a cusped orientable hyperbolic 4-manifold $\mathcal{X}$ of finite volume.*

Proof. As stated in Proposition 4.6, $\mathcal{R}$ has a total of five disjoint totally geodesic boundary components, four of which (the small ones) are isometric

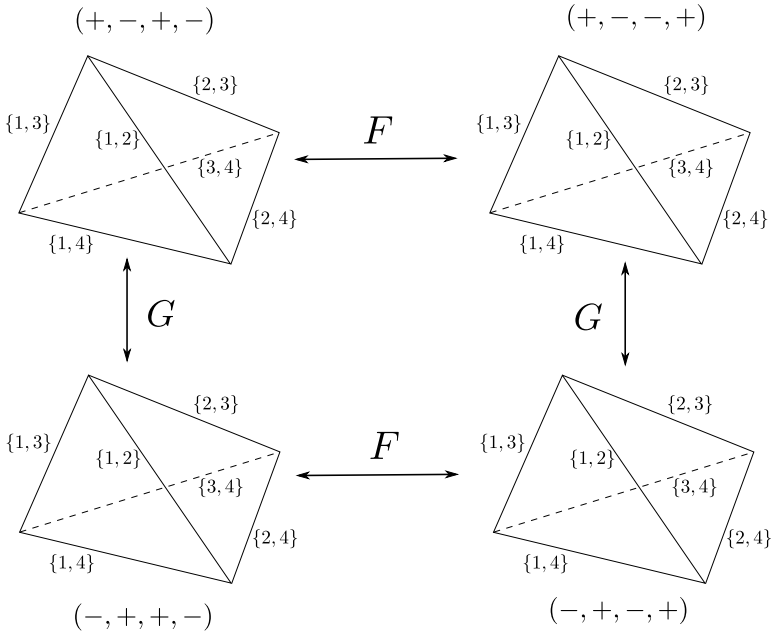

Figure 4.7: Triangulation encoding the large boundary component M of $\mathcal{X}$. The map F pairs the two top faces of the indicated tetrahedra, sending edges labeled $\{1,2\}$ to edges labeled $\{1,2\}$, and edges labeled $\{i,3\}$ to edges labeled $\{i,4\}$ for $i = 1,2$. The map G pairs the bottom faces, sending edges labeled $\{3,4\}$ to edges labeled $\{3,4\}$, and edges labeled $\{1,i\}$ to edges labeled $\{2,i\}$ for $i = 3,4$. All pairings are orientation reversing.

to each other, so it suffices to pair these four components together isometrically. We may for instance consider the orientation reversing map $K : \mathbb{R}^4 \to \mathbb{R}^4$ defined by

$$K(x, y, z, w) = (-y, -x, z, w).$$

We use it to pair the boundary components of $\mathcal{R}$ with labels $\pm(+,+,+,+)$ and $\pm(+,+,-,-)$, obtaining an orientable 4-manifold $\mathcal{X}$. The hyperbolic structure on $\mathcal{R}$ extends to one on $\mathcal{X}$, which has one totally geodesic boundary component isomorphic to M. The manifold $\mathcal{X}$ is tessellated by two regular ideal hyperbolic 24-cells, and has volume $2 \cdot v_m$, where $v_m = 4\pi^2/3$ is the volume of the regular ideal hyperbolic 24-cell. □

Chapter 5

The boundary manifold as link complement

In this chapter we will exhibit a presentation of the geometrically bounding manifold M as link complement in S^3. Recall from Section 3.2 that it is possible to associate a presentation as a partially framed link to every orientable manifold built from a triangulation $\mathcal{T}$. We have seen in the previous chapter that the bounding manifold M is constructed from a triangulation $\mathcal{T}$ with four tetrahedra as in Figure 4.7.

The presentation of M as partially framed link L is shown in Figure 5.1 (top). The zero-framed components are labeled F_i, for $i = 1, \ldots, 5$. The four components labeled y, r, g, b correspond to the large cusps of M, while the components labeled s_i, for $i = 1 \ldots, 4$ correspond to the small ones.

We wish to eliminate the framed components F_i by applying blow-ups/downs and handle-slides. We begin by applying a handle-slide of F_5 over F_4, modifying L to the link of Figure 5.1 (bottom). For simplicity, we continue to label the new framed component F_5. Notice that the component labeled r is unlinked from all the framed components except F_5.

As a second step, we get rid of the framed components F_i, for $i = 1, \ldots, 4$. We use the local move represented in Figure 5.2. This move can be viewed as a composition of two moves. The first is a twist on an unknotted non-framed component, which does not change the underlying manifold as shown in page 265 of [15]. The second is a topological blow-down.

We apply this local move within small balls that encircle the unknotted framed components F_i, $i = 0, \ldots, 4$ and the unknotted non-framed components s_i, $i = 1, \ldots, 4$. The role of l is played by the components labeled F_i, while the role of c is played by the components labeled s_i. We choose the directions of the twist in such a way that that clockwise (resp. counterclockwise) half-twists of the coloured components become counterclockwise (resp. clockwise). In other words we choose the twists in order to minimize the linking number of the coloured components.

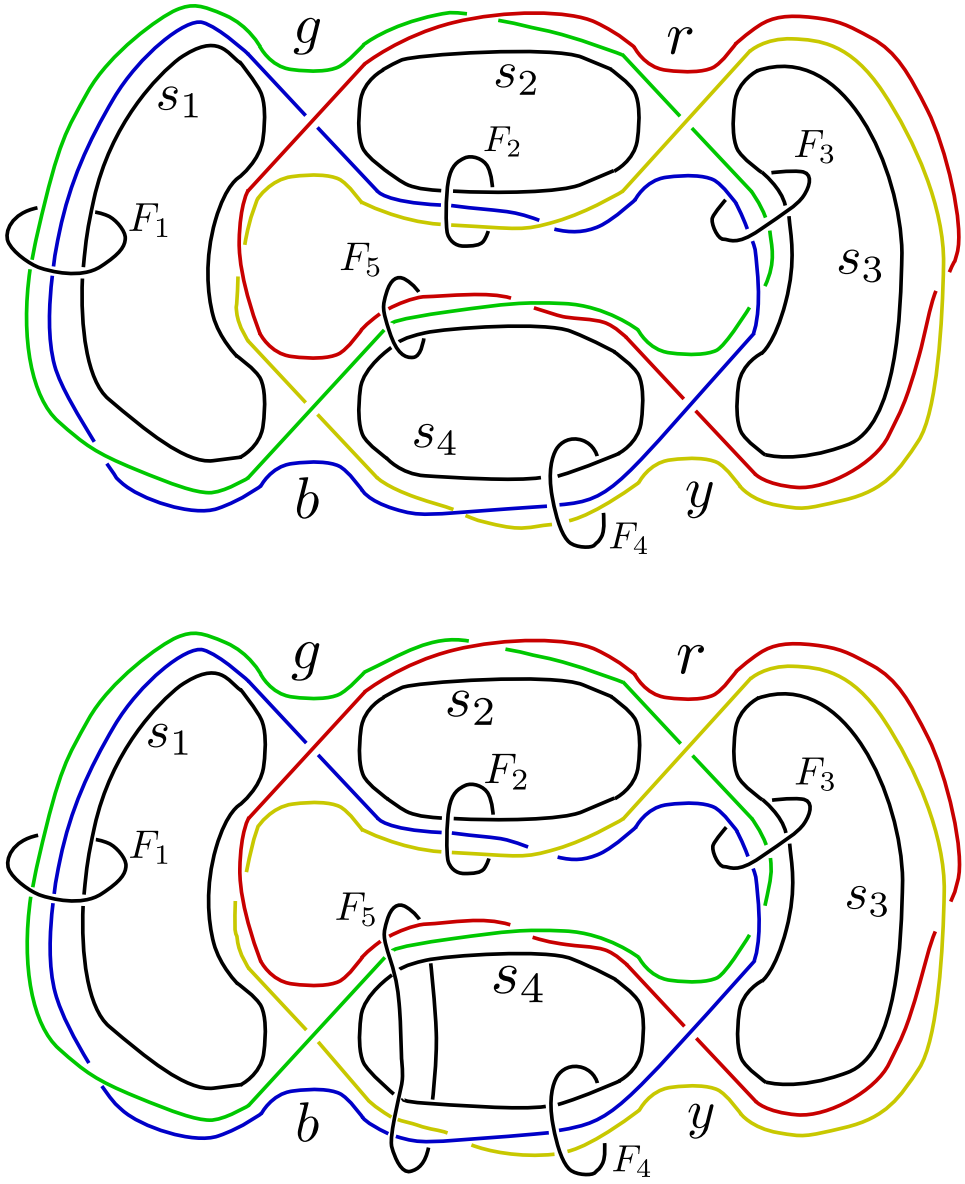

Figure 5.1: Presentations of the geometrically bounding manifold M as a partially framed link.

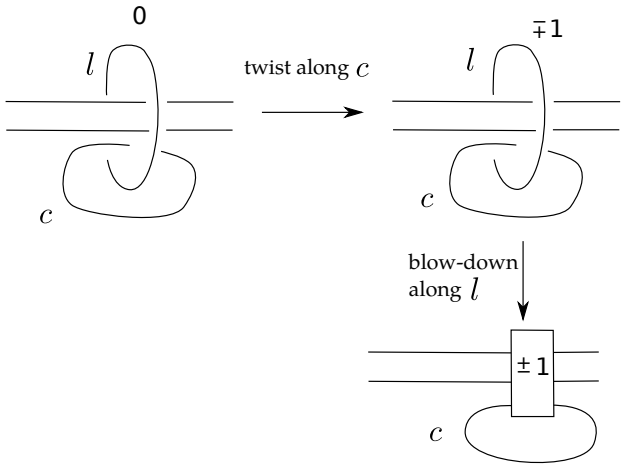

Figure 5.2: Local twist along an unknotted zero-framed component l. This move is the result of a twist along an unknotted, non-framed component c, which changes to ∓ 1 the framing on l, followed by a blow-down on l. The rectangle labeled by ± 1 represents a full twist of the strands that cross it. This twist is counter-clockwise (resp. clockwise) if the twist along c is chosen to be clockwise (resp. clockwise).

The result of these moves is shown in Figure 5.3. There is just one component, F_5, with zero framing, so what we have now is a presentation of the manifold M as a link complement in $S^2 \times S^1$. In fact the components labeled y, r, g, b form a pure braid in a solid torus $D^2 \times S^1 \subset S^2 \times S^1$. The components labeled s_1, s_2, s_3, s_4 are linked with the components labeled y, g, b, but not with r.

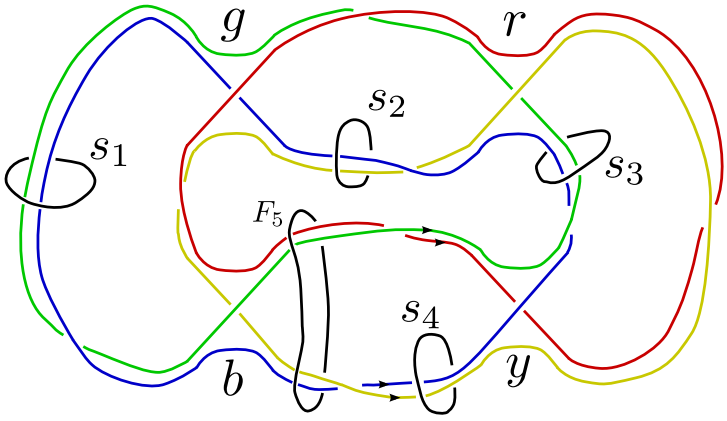

Figure 5.3: Presentation of the geometrically bounding manifold M as a link complement in $S^2 \times S^1$.

The braid formed by the components labeled y, r, g, b is represented in

Figure 5.4. The strand labeled r winds once around the sub-braid formed by the components y, g, b. As a consequence of this fact, we see that the framed link of Figure 5.3 is isotopic to the framed link of Figure 5.5.

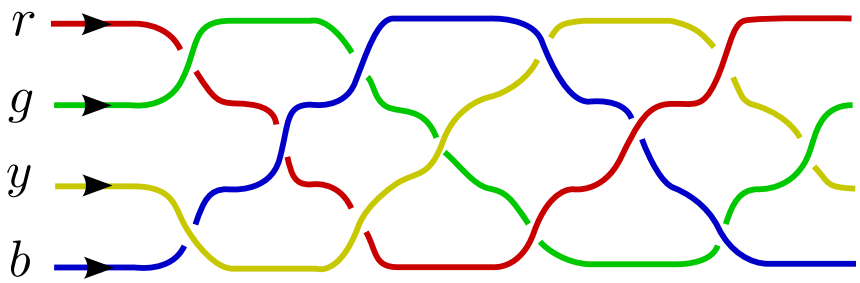

Figure 5.4: Pure braid in $S^2 \times S^1$ formed by the coloured components.

We can now proceed to remove the last framed component. We use a sequence of local moves, which all take place within the region highlighted by a dashed line in Figure 5.5. We begin by performing a clockwise twist on the component labeled r, which changes to -1 the framing on F_5, unlinking it from all the components except r. A blow-down along F_5 allows us to remove this last framed component. Notice that the blow-down twists the components labeled by y, g and b by a full clockwise twist (see Figure 5.6).

The result of this move is shown in Figure 5.7. As a final step, we apply a counter-clockwise twist along the component labeled r. This moves removes the crossings to the left of the component labeled r, and simplifies the link complement to the one of Figure 5.8.

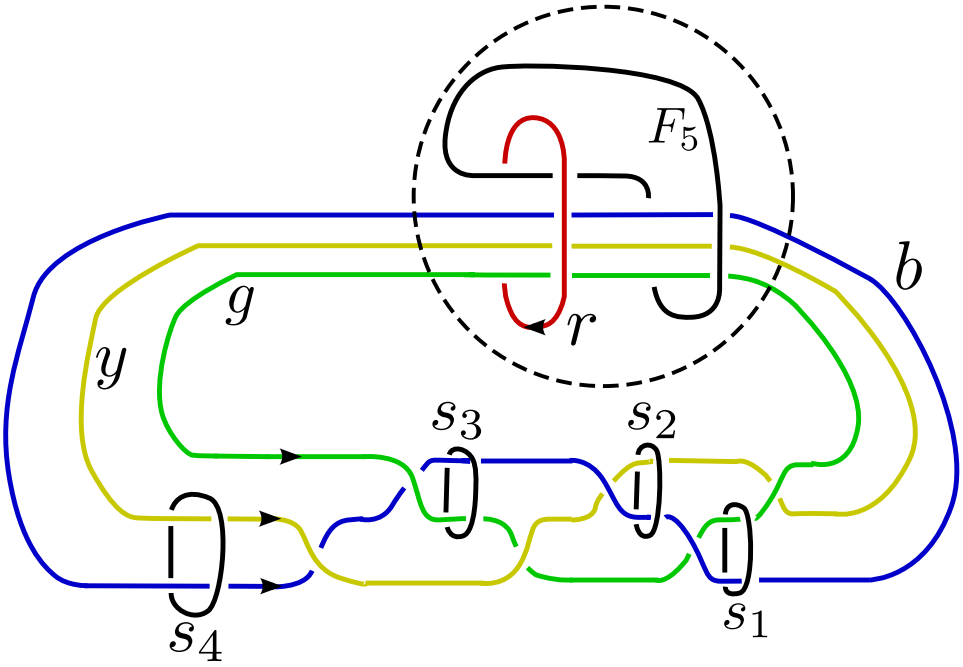

Figure 5.5: Modified presentation of the bounding manifold as link complement in $S^2 \times S^1$.

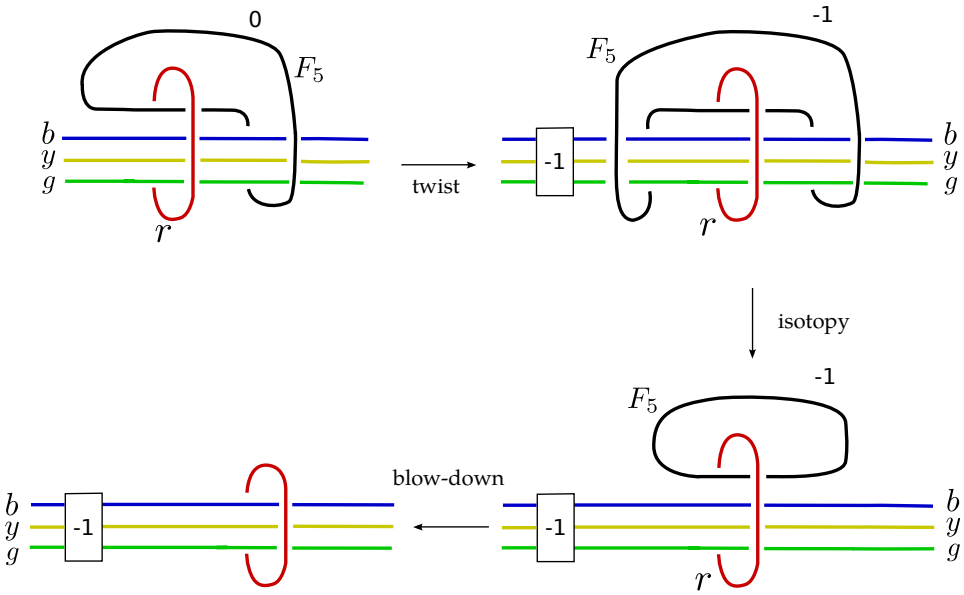

Figure 5.6: Kirby moves removing the last framed component.

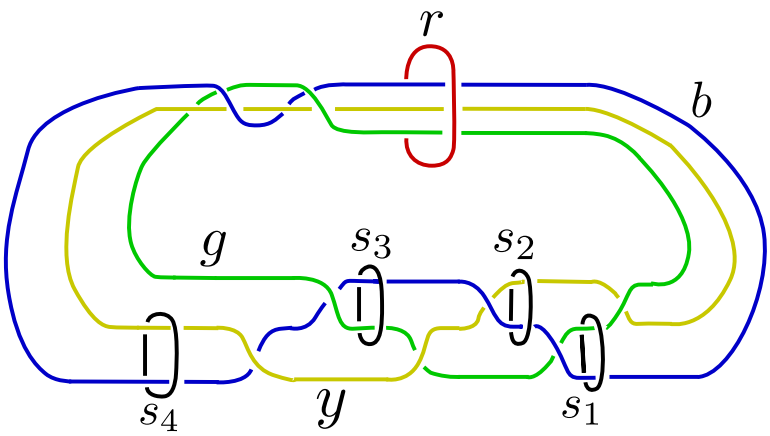

Figure 5.7: Presentation of the bounding manifold as link complement in S^3.

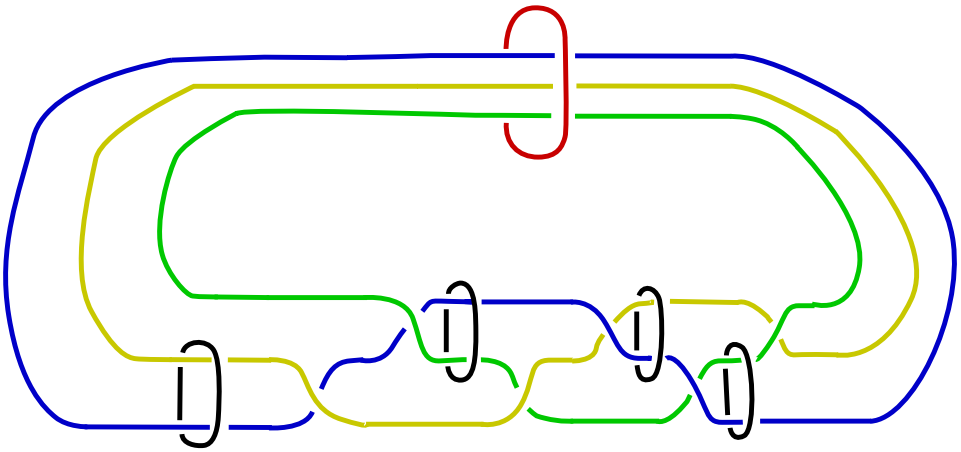

Figure 5.8: Simplified presentation of the bounding manifold as link complement in S^3.

Chapter 6

Simple hyperbolic 4-manifolds

In this chapter we will construct two new examples of non-compact hyperbolic 4-manifolds with low volume and number of cusps. Both of them are constructed by pairing isometrically the facets of copies of the regular ideal hyperbolic 24-cell $\mathcal{C}$.

6.1 A minimal volume hyperbolic 4-manifold with two cusps

The volume spectrum of hyperbolic 4-manifolds is known to be the set of positive integral multiples of $v_m = 4\pi^2/3$ [14]. This is exactly the volume of the regular ideal hyperbolic 24-cell $\mathcal{C}$, so we may expect to build examples of cusped hyperbolic 4-manifolds of minimal volume by pairing the facets of one copy of $\mathcal{C}$. This has been done in [14] by Ratcliffe and Tschantz, who produced a list of 1171 manifolds of the form $\mathbb{H}^4/\Gamma$ where Γ is a torsion-free subgroup of minimal index in the congruence-two subgroup Γ^4_2 of the group Γ^4 of integral Lorentzian 5×5 matrices. All the resulting manifolds have either five or six cusps.

In this section we will exhibit a hyperbolic 4-manifold of minimal volume with only two cusps. To our knowledge, this is the lowest number of cusps realized by a known minimal volume hyperbolic 4-manifold.

We begin considering a 24-cell $\mathcal{C}$ and we pair each green facet with its opposite using the antipodal map $v \mapsto -v$. We denote with $\mathcal{C}/\sim$ the resulting nonorientable manifold. The red/blue coloring of the boundary 3-strata induces one on $\mathcal{C}/\sim$.

As a second step, we pair the red facets (those with an even number of minus signs) through the map $H : \mathbb{R}^4 \to \mathbb{R}^4$ defined by

$$H(x, y, z, w) = (-x, -y, z, w).$$

Let us call $\mathcal{A}$ the resulting nonorientable space.

Proposition 6.1. *The space $\mathcal{A}$ is a hyperbolic 4-manifold with eight cusps whose sections fall into two homothety classes: there are four* mute *cusps and four* non-mute *cusps, as defined below. Moreover, it has two disjoint totally geodesic boundary components X and Y, each isomorphic to the complement of the minimally twisted 6-chain link of Figure 6.1.*

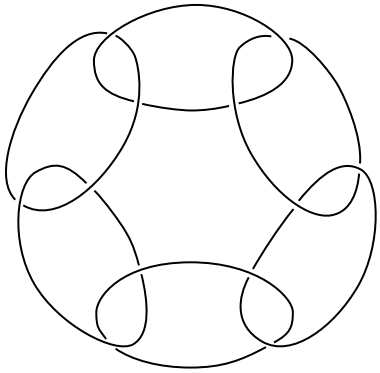

Figure 6.1: The minimally twisted 6-chain link. The boundary of $\mathcal{A}$ consists of two disjoint copies of its exterior.

Proof. The cusp sections of $\mathcal{A}$ are obtained by pairing with the map H the faces of the cusp sections of the manifold $\mathcal{C}/\sim$, and are represented in Figure 6.2.

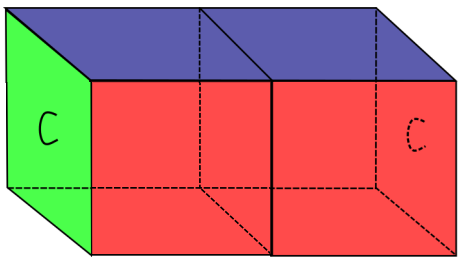

Figure 6.2: A fundamental domain for the cusp section of the manifold $\mathcal{A}$. The opposite faces of each cube share the same colour, and the green faces are identified in pairs.

There are 12 such cusps, one for each couple of opposite vertices of the 24-cell. Each cusp is labeled with a 4-uple of $+, -, 0$ symbols with two 0 entries, defined up to change in signs (*i.e.* changing every $+$ sign to a $-$ sign and every $-$ sign to a $+$ sign). To mantain a rigorous notation, we will use square parentheses to highlight that we are speaking of equivalence classes. The cusps labeled $[(+,+,0,0)]$, $[(+,-,0,0)]$, $[(0,0,+,-)]$ and $[(0,0,+,+)]$

are fixed by the map H, therefore each of them corresponds to one cusp of $\mathcal{A}$. We label them respectively m_1, n_1, m_2 and n_2. Figure 6.3 shows a fundamental domain for their cusp section, together with the identifications on the green and the red faces.

We call these the *mute* cusps of $\mathcal{A}$, as they have only one boundary component, obtained by glueing together the four blue faces along the edges. This boundary component is isomorphic to a torus, obtained by identifying opposite sides of a square of sidelength two.

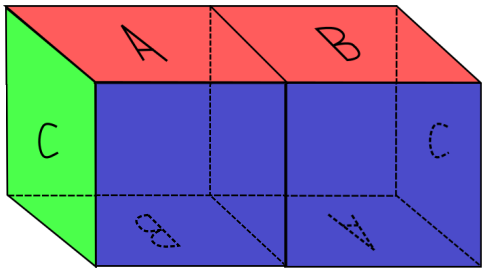

Figure 6.3: A fundamental domain for the mute cusps of $\mathcal{A}$. The letters show the identifications between green and red faces.

The other four cusps, labeled a, b, c and d, are obtained from the following pairings between the cusps of $\mathcal{C}/\sim$, induced by the map H:

$$\begin{aligned} a &: [(+,0,+,0)] \leftrightarrow [(-,0,+,0)], \\ d &: [(0,+,0,+)] \leftrightarrow [(0,-,0,+)], \\ b &: [(+,0,0,+)] \leftrightarrow [(-,0,0,+)], \\ c &: [(0,+,+,0)] \leftrightarrow [(0,-,+,0)]. \end{aligned}$$

The resulting cusp section is represented in Figure 6.4. These cusps have two boundary components, once again isomorphic to a square torus of sidelength two. In all the above cases, the cusp sections are Euclidean 3-manifolds. Therefore $\mathcal{A}$ possesses a hyperbolic structure with totally geodesic boundary.

Each of the boundary components of $\mathcal{A}$ is obtained by glueing together along their faces four of the blue octahedral facets of the 24-cell $\mathcal{C}/\sim$. Each blue octahedral facet of the 24-cell possesses a red/green checkerboard coloring on its triangular 2-faces, analogous to the one described in the proof of Proposition 4.6.

The boundary components of $\mathcal{A}$ can be described as the result of a double mirroring of a regular ideal hyperbolic octahedron, as in Figure 6.5 (top), where the first mirroring is performed along the green faces and the second along the red. The mirroring on the green faces is the result of the pairing of the green octahedral facets of the 24-cell, which is performed with the antipodal map $v \mapsto -v$. The mirroring on the red faces is the result of the pairing of the red facets, which is performed by the affine map H.

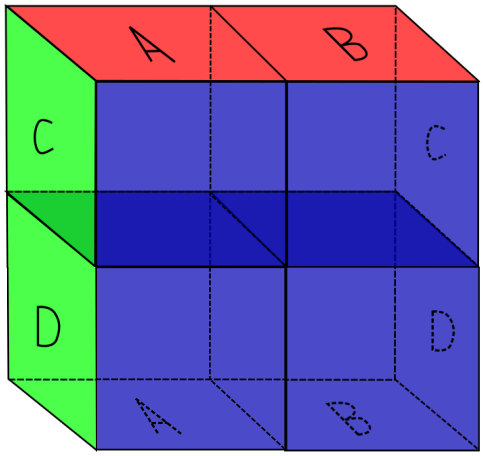

Figure 6.4: A fundamental domain for the non-mute cusps of $\mathcal{A}$. Letters show the identifications between green and red faces.

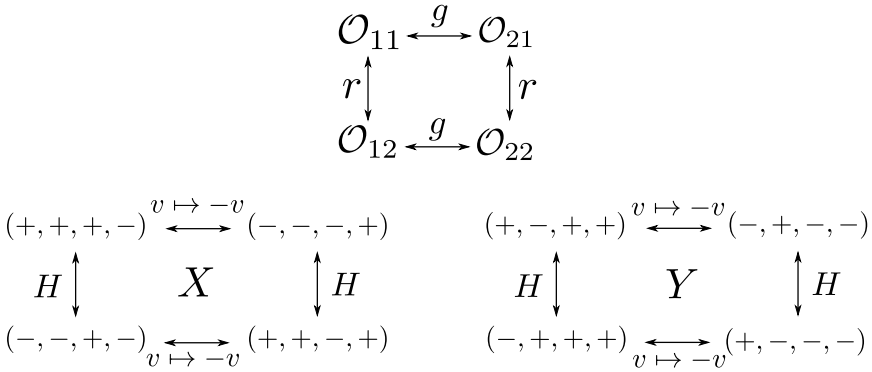

Figure 6.5: Presentations of the boundary components of $\mathcal{A}$ as a double mirroring of a regular ideal hyperbolic octahedron $\mathcal{O}$. Labels show which 3-strata of the 24-cell compose each boundary component. The antipodal map identifies the green faces, while H identifies the red ones.

As proven in [6], these boundary components are isomorphic to the exterior of the minimally twisted 6-chain link, represented in Figure 6.1. □

The exterior M_L of the minimally twisted 6-chain link represented in Figure 6.1 has two isometries W and V, obtained by reflecting respectively in the green and the red faces. The isometry W (resp. V) acts on the square diagram of Figure 6.5 (top) interchanging $\mathcal{O}_{1i}$ with $\mathcal{O}_{2i}$ (resp. $\mathcal{O}_{i1}$ with $\mathcal{O}_{i2}$). In the case of the boundary components X and Y of $\mathcal{A}$, the isometries W and V are induced respectively by the antipodal map $v \mapsto -v$ and the affine map E on $\mathcal{C}$.

Proposition 6.2. *Every isometry of M_L preserves its decomposition as a union of four copies of the ideal hyperbolic octahedron $\mathcal{O}$. There is an exact sequence*

$$0 \to \mathbb{Z}_2 \oplus \mathbb{Z}_2 \to \mathrm{Isom}(M_L) \to \mathrm{Isom}(\mathcal{O}) \to 0.$$

Where $\mathbb{Z}_2 \oplus \mathbb{Z}_2$ is the group generated by W and V.

Proof. The four octahedra O_{ij} represent the canonical Epstein-Penner decomposition of M_L, and are therefore preserved by any isometry. Every isometry of M_L is the composition of an isometry in $\mathbb{Z}_2 \oplus \mathbb{Z}_2$ with one which fixes the octahedron $\mathcal{O}_{11}$. This defines the map onto $\mathrm{Isom}(\mathcal{O}_{11}) \cong \mathrm{Isom}(\mathcal{O})$. Its kernel is precisely the group generated by W and V. □

6.1.1 Gluing of the boundary components

As a last step to obtain a manifold with no boundary, we need to glue the boundary components X and Y of $\mathcal{A}$ together using an appropriate isometry $\phi : X \to Y$. As a consequence of Proposition 6.2, to encode ϕ we need to specify the choice of two octahedra $\mathcal{O}_1$ and $\mathcal{O}_2$ from X and Y respectively, together with an isometry from $\mathcal{O}_1$ to $\mathcal{O}_2$. We choose $\mathcal{O}_1$ as the octahedron with labeling $(+,+,+,-)$ and $\mathcal{O}_2$ as that with labeling $(+,-,+,+)$. This choice is purely arbitrary and, as a consequence of Proposition 6.2, does not affect the argument which will follow.

Each of the octahedra $\mathcal{O}_i$ has two opposite ideal vertices belonging to the mute cusps, and the remaining four belonging to a, b, c and d as in Figure 6.6. Notice that the boundary components of the mute cusps labeled m_i belong to X, while those labeled n_i belong to Y. Each non-mute cusp has one boundary component on X and one on Y. Furthermore the cusps labeled a and d always lie on opposite vertices of the octahedra, as do those labeled b and c.

To define ϕ, we choose the map from $\mathcal{O}_1$ to $\mathcal{O}_2$ which pairs the vertices in the following way:

$$\begin{gathered} \mathcal{O}_1 \xrightarrow{\phi} \mathcal{O}_2 \\ m_1 \mapsto b \end{gathered}$$

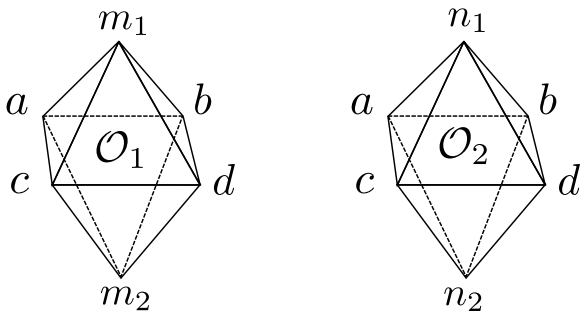

Figure 6.6: Model for the octahedra O_i. Each vertex is labeled with the cusp to which it belongs.

$$\begin{aligned} m_2 &\mapsto c \\ b &\mapsto d \\ c &\mapsto a \\ a &\mapsto n_1 \\ d &\mapsto n_2. \end{aligned}$$

Proposition 6.3. *Let $\mathcal{G}$ be the manifold*

$$\mathcal{A}/(x \sim \phi(x))$$

obtained by gluing the boundary components X and Y together using ϕ as defined above. The manifold $\mathcal{G}$ has a hyperbolic structure with two cusps. Its hyperbolic volume is equal to $v_m = 4\pi^2/3$.

Proof. The hyperbolic structure of $\mathcal{G}$ is inherited from that of $\mathcal{A}$, since we are glueing by an isometry its two disjoint totally geodesic boundary components. The effect of this glueing is to concatenate the cusps of $\mathcal{A}$ along their boundary components in two groups of four, with the mute cusps at the ends and the non-mute cusps in the middle, as in Figure 6.7.

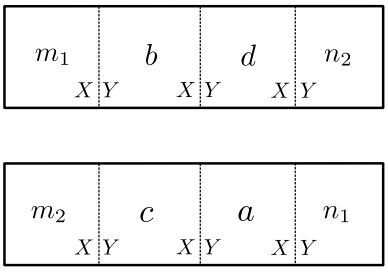

Figure 6.7: Cusps of $\mathcal{G}$ as a result of glueing the cusps of $\mathcal{A}$. The letters in the middle of the squares indicate the cusps of $\mathcal{A}$. Dotted lines indicate their boundary components.

Since $\mathcal{G}$ is obtained by pairing the facets of one regular ideal hyperbolic 24-cell, it has exactly the same volume $v_m = 4\pi^2/3$. □

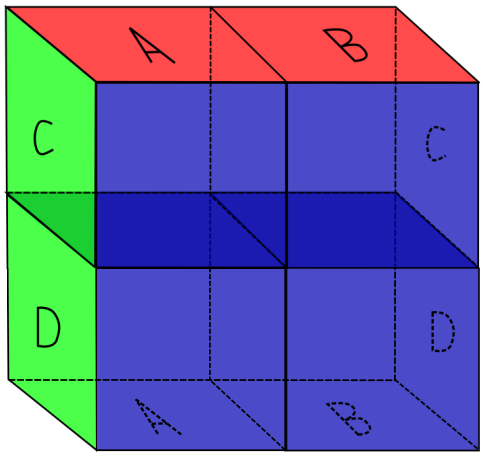

Figure 6.8: A fundamental domain for the cusp sections of $\mathcal{A}$. Letters show the identifications between green and red faces.

6.2 A one-cusped hyperbolic 4-manifold

Kolpakov and Martelli [6] have recently built the first example of hyperbolic 4-manifold with one (toric) cusp. Their example has volume equal to $4 \cdot v_m$. In this section we will construct an example of non-orientable hyperbolic 4-manifold with one toric cusp and volume equal to $2 \cdot v_m$. To our knowledge, this manifold has the lowest volume among the known one-cusped hyperbolic 4-manifolds.

We begin by considering two copies $\mathcal{C}_1$ and $\mathcal{C}_2$ of the regular ideal hyperbolic 24-cell $\mathcal{C}$, with opposite orientations, and we glue them together along their green facets via the map induced by the identity on $\mathcal{C}$. We subsequently glue each red facet of $\mathcal{C}_i$ to the opposite face of $\mathcal{C}_i$ using the antipodal map $v \mapsto -v$.

Let us call $\mathcal{D}$ the resulting nonorientable space.

Proposition 6.4. *The space $\mathcal{D}$ is a hyperbolic manifold with twelve cusps whose sections are all isometric to each other. It has four disjoint totally geodesic boundary components, each isomorphic to the exterior of the minimally twisted* 6*-chain link of Figure 6.1.*

Proof. The cusp sections of $\mathcal{D}$ are obtained by glueing along their red boundary faces the cusp sections of a mirrored 24-cell $\mathcal{S}$ of Definition 4.2. The glueing is induced by the antipodal map on each $\mathcal{C}_i$. The resulting cusp section is represented in figure 6.8.

There are 12 such cusps, one for each pair of opposite vertices of the 24-cell, naturally labeled by a 4-uple of $0, +, -$ symbols with two zero entries, defined modulo changes in signs (changing every $+$ sign to a $-$ sign and

every $-$ sign to a $+$ sign). To simplify notations we will use the following labelings:

$$a_1 = [(+,+,0,0)],\ a_2 = [(+,-,0,0)],$$
$$d_1 = [(0,0,+,+)],\ d_2 = [(0,0,+,-)],$$
$$b_1 = [(+,0,+,0)],\ b_2 = [(+,0,-,0)],$$
$$e_1 = [(0,+,0,+)],\ e_2 = [(0,+,0,-)],$$
$$c_1 = [(+,0,0,+)],\ c_2 = [(+,0,0,-)],$$
$$f_1 = [(0,+,+,0)],\ f_2 = [(0,1,-1,0)].$$

The cusps sections are Euclidean 3-manifolds, isometric to a product $T \times I$, where T is a square torus of sidelength two and I is a unit interval. Therefore $\mathcal{A}$ possesses a hyperbolic structure with totally geodesic boundary.

Each boundary 3-stratum is obtained from the gluings of four of the blue octahedral facets of the 24-cells $\mathcal{C}_1$ and $\mathcal{C}_2$ along their triangular 2-faces, and is representable as a double mirroring of an octahedron with a red/green checkerboard coloring as in Figure 6.9. Indeed, the mirroring on the green faces glues a blue octahedral facet O_1 of $\mathcal{C}_1$ to the correponding facet O_2 of $\mathcal{C}_2$, while the mirroring on the red faces glues a blue octahedral facet O_i to its opposite $-O_i$ in $\mathcal{C}_i$. These boundary components are naturally labeled as the *blue* facets of the 24-cell, *i.e.* with a 4-uple of $+,-$ symbols, defined up to change in signs (changing every $+$ sign to a $-$ sign and every $-$ sign to a $+$ sign). To simplify notations, we will use the following labelings:

$$B_1 = [(-,+,+,+)],\ B_2 = [(+,-,+,+)],$$
$$B_3 = [(+,+,-,+)],\ B_4 = [(+,+,+,-)].$$

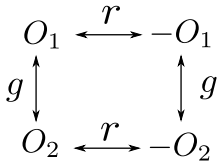

Figure 6.9: Presentation of a boundary component of $\mathcal{D}$. It is made up of blue facets O_1 and O_2 from $\mathcal{C}_1$ and $\mathcal{C}_2$, both corresponding to the same facet O of $\mathcal{C}$, together with their opposites $-O_1$ and $-O_2$.

□

6.2.1 Glueing of the boundary components

We now need to identify in pairs the boundary components B_i, for $i = 1, \ldots, 4$ to produce a manifold with no boundary. We choose to pair B_3 with B_1 via an isometry ϕ_1 and B_4 with B_2 via an isometry ϕ_2. As in the previous section, to define the maps ϕ_i, $i = 1, 2$, we must choose one octahedron from the domain and one from the codomain, and then specify

how we pair them. As a consequence of Proposition 6.2, the first choice does not affect the argument which will follow. We can choose, for example, for ϕ_1 (resp. ϕ_2) to pair the octahedral facet of $\mathcal{C}_1$ labeled $(-,+,+,+)$ (resp. $(+,-,+,+)$) with the facet of $\mathcal{C}_1$ labeled $(+,+,-,+)$ (resp. $(+,+,+,-)$). These octahedra have ideal vertices belonging to different cusps of $\mathcal{D}$ as shown in Figure 6.10.

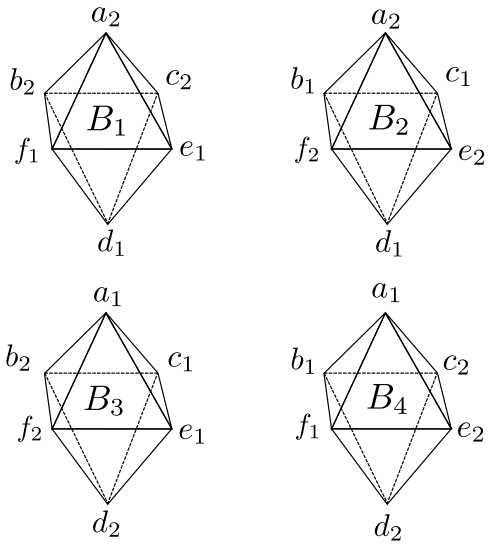

Figure 6.10: Correspondence between cusps of $\mathcal{D}$ and ideal vertices of the octahedra which constitute the boundary components B_i.

To choose the glueing maps ϕ_1 and ϕ_2, we choose the following pairings between the vertices:

$$\begin{array}{cc} B_4 \xrightarrow{\phi_2} B_2 & B_3 \xrightarrow{\phi_2} B_1 \\ a_1 \mapsto c_1 & a_1 \mapsto b_2 \\ d_2 \mapsto f_2 & d_2 \mapsto e_1 \\ c_2 \mapsto e_2 & b_2 \mapsto f_1 \\ f_1 \mapsto b_1 & e_1 \mapsto c_2 \\ b_1 \mapsto a_2 & f_2 \mapsto a_2 \\ e_2 \mapsto d_1 & c_1 \mapsto d_1 \end{array}$$

Proposition 6.5. *Let $\mathcal{H}$ be the non-orientable manifold*

$$\mathcal{D}/(x \sim \phi_i(x))$$

obtained by glueing in pairs the boundary components B_i using ϕ_1 and ϕ_2 as defined above. $\mathcal{H}$ has a hyperbolic structure with total volume equal to $2 \cdot v_m$ and one toric cusp.

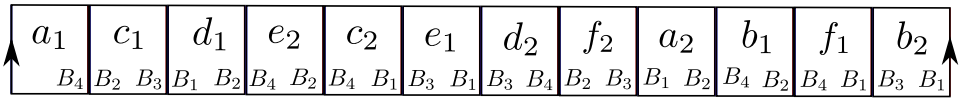

Figure 6.11: The cusp of $\mathcal{H}$ as concatenation of the cusps of $\mathcal{D}$. Vertical edges mark the identifications induced on the boundary components B_i by the maps ϕ_1 and ϕ_2. The cusp shape is that of a torus obtained by identifying opposite faces of a $2 \times 2 \times 12$ rectangular parallelepiped.

Proof. The hyperbolic structure of $\mathcal{D}$ induces one on $\mathcal{H}$. The 12 cusp sections of $\mathcal{D}$ are concatenated along their boundary components to form the only cusp of $\mathcal{H}$ as in Figure 6.11.

The volume is $2 \cdot v_m$, because $\mathcal{H}$ is obtained by pairing the facets of two copies of the regular ideal hyperbolic 24-cell. □

Remark 6.6. The orientable double cover of the manifold $\mathcal{H}$ of Proposition 6.5 is the example of one cusped hyperbolic 4-manifold constructed by Kolpakov and Martelli in [6].

Bibliography

[1] R. Benedetti, C. Petronio: *Lectures on hyperbolic geometry*, Universitext, Springer (1992)

[2] F. Costantino, R. Frigerio, B. Martelli, C. Petronio: *Triangulations of 3-manifolds, hyperbolic relative handlebodies, and Dehn filling*, Comm. Math. Helv. 82 (2007), 903-934

[3] R. Fenn C. Rourke: *On Kirbys calculus of links*, Topology 18 (1979), 1-15

[4] G. W. Gibbons: *Tunneling with a negative cosmological constant*, Nuclear Phys. B, 472 (1996) 683-708

[5] R. Kirby: *A calculus for framed links in* S^3 , Invent. Math. 45 (1978), 35-56

[6] A. Kolpakov, B. Martelli: *Hyperbolic 4-manifolds with one cusp*, Geom. & Funct. Anal. 23 (2013), 1903-1933

[7] A. Kolpakov, B. Martelli, S. Tschantz: *Some hyperbolic three-manifolds that bound geometrically*, arXiv:1311.2993

[8] W. B. R. Lickorish: *A representation of orientable combinatorial 3-manifolds*, Ann. of Math. 76 (1962), 531-540

[9] W. B. R. Lickorish: *An introduction to knot theory*, Graduate Texts in Mathematics, Springer (1997)

[10] D. D. Long, A. W. Reid: *On the geometric boundaries of hyperbolic 4-manifolds*, Geometry & Topology, Volume 4 (2000) 171-178

[11] D. D. Long, A. W. Reid: *Constructing hyperbolic manifolds which bound geometrically*, Math. Research Lett. 8 (2001), 443-456

[12] B. Martelli, *A finite set of local moves for Kirby calculus*, arXiv:1102.1288

[13] J. G. Ratcliffe, S. T. Tschantz: *Gravitational instantons of constant curvature*, Classical and Quantum Gravity, 15 (1998) 2613-2627

[14] J. G. Ratcliffe, S. T. Tschantz: *The volume spectrum of hyperbolic* 4-*manifolds*, Experimental J. Math. 9 (2000) 101-125

[15] D. Rolfsen: *Knots and links*, AMS Chelsea Publishing, American Mathematical Society (2003)

[16] W. P. Thurston: 3-*dimensional manifolds, Kleinian groups and hyperbolic geometry*, Bulletin of the American Mathematical Society, Volume 6, Number 3, May 1982

[17] W. P. Thurston: *The Geometry and Topology of* 3-*manifolds*, mimeographed notes, Princeton, 1979

[18] A. H. Wallace: *Modifications and cobounding manifolds*, Canad. J. Math. 12 (1960), 503-528